Bulletin of the Mineral Research and Exploration

http://bulletin.mta.gov.tr

Petrographic characteristics of deep marine turbidite sandstones of the Upper Cretaceous Tanjero Formation, Northwestern Sulaimaniyah, Iraq: Implications for provenance and tectonic setting

Hasan ÇELİK[a*] and Hemin Muhammad HAMA SALİH[b]

[a]*Fırat University, Engineering Faculty, Department of Geological Engineering, 23119, Elazığ, Turkey*
[b]*Ministry of Higher Education and Scientific-Research, Sulaimaniyah, Iraq*

Research Article

Keywords:
Sedimentary petrography, provenance, Tanjero Formation, Northwestern Sulaimaniyah, Iraq.

ABSTRACT

This study was carried out to determine the sedimentary provenance of Upper Cretaceous turbidites of Tanjero Formation. The sandstone portion of the unit has been examined based on field and laboratory studies. Seven sections were measured and described in detail on the perfectly cropped out part of the unit at the southern limb of the Sulaimaniyah Syncline. The thickness of the measured sections varies from 120 m to 192 m. The measured sections start from the top of the underlying Shiranish Formation to the syncline axis in the Tanjero Formation. For petrographic analysis sixty-nine representative rock samples were collected. Modal analysis and ternary diagrams point out that, the sandstones are calclithite (litharenite), very fine to medium grained in size consisting of chert, siltstone, mudstone, radiolarian chert and radiolarian mudstone fragments, angular to subangular in shape, very poorly to moderately sorted, transported over short distances and represent submature stage. Grain contact types and high contact index (4.7) indicate moderate to tightly packing, moderate compaction. Transported broken neritic fossil shells, moderately rounded glauconite grains, and undefinable fossils in the altered carbonate rock fragments indicate that the tectonic provenance, lithic recycle category, composed of not only the clastics as interpreted in previous studies derived from Lower Cretaceous Qulqula (radiolarian) Formation which represents deep marine, but also it revealed that a sedimentary formation must also exist in the source area, which is the Lower Cretaceous Balambo Formation.

Received Date: 14.11.2019
Accepted Date: 19.09.2020

1. Introduction

Northern part of Iraq is an oil field area, there are many researches which are summarized in this part of the paper that majority of them were done on carbonate-sand some on clastic rocks excluding provenance analysis.

Provenance types contribute distinctive detritus preferentially to associate sedimentary rocks. For this reason, clastic detrital components save valuable data on the provenance and pattern in which the sediments were transported, especially after modification of the original detritus by the interaction of physical and chemical processes such as weathering, erosion transportation and paleoclimate (Johnson, 1976; Dickinson, 1988). Turbidites also contain important information for interpreting both the compositional tectonic setting and evolution of the continental crust that can be linked to the depositional environment

Citation Info: Çelik, H., Hama Salih, H. M. 2021. Petrographic characteristics of deep marine turbidite sandstones of the Upper Cretaceous Tanjero Formation, Northwestern Sulaimaniyah, Iraq: Implications for provenance and tectonic setting. Bulletin of the Mineral Research and Exploration 164, 11-38.
https://doi.org/10.19111/bulletinofmre.800132

**Corresponding author: Hasan ÇELİK, hasancelik@firat.edu.tr*

(Raymond, 1995; Cingolani et al., 2003). Petrographic studies show that clastic rocks can be used for classification the provenance (Dickinson et al., 1983; Bordy et al., 2004; Armas et al., 2014).

Studies of sedimentary petrography and palaeo flow direction for provenance analysis are important to refine depositional environment for assessing reservoir properties of the hydrocarbon reservoirs (Rieser et al., 2005; Mange and Morton 2007; Li et al., 2012; Ghosh et al., 2012).

So far the geological studies of the Tanjero Formation were carried out by Dunnington (1958), Bellen et al. (1959), Kassab (1975), Al-Mehaidi (1975), Abdel-Kireem (1986*a*, 1986*b*), Jaza (1992), Minas (1997), Karim (2004, 2007, 2010), Karim and Surdashy (2005*a*, 2005*b*), Sharbazheri (2007, 2010), Karim et al. (2012, 2014), Lawa et al. (2013, 2017) mainly in the manner of paleontology, lithostratigraphy, biostratigraphy, sequence stratigraphy, sedimentology, basin analysis, and lithofacies but despite these studies, mainly not published in international SCI journals, the petrography and mineralogical composition of the turbidites have not been studied seriously yet and still poorly understood.

Zagros Suture Zone is the one of the main tectonically active part of the area. In the recent decade some tectonic and evolution studies of Neotethys were done by Alavi (2004, 2007), Karim and Taha (2009), Lawa et al. (2013), Sissakian (2013), Malekzade et al. (2016), Motaghi et al. (2017), Moradpour et al. (2017), Koshnaw et al. (2018, 2019).

The Tanjero Formation crops out in the northern Iraq province throughout Iran border (Figure 1 and 2) consisting of low density deep marine fan turbidites. Around Sulaimaniyah, the unit consisting of mainly sandstone, siltstone and shale were studied to interpret the provenance. Elsewhere in northern Iraq some researchers (e.g. Karim 2004, 2007, 2010; Karim et al., 2012; 2014) state that the unit comprises conglomerate and limestone indicating the shallow water rocks of the formation. However, the unit conformably overlies marly Shiranish Formation (lower Campanian-Maastrichtian) in general, but in some places an interfingering relations can be seen between these two formations (Figure 3). The Tanjero Formation is conformably covered by upper Maastrichtian-middle Paleocene Kolosh Formation (Karim, 2010).

A large-scale northwest-southeast trending anticline and syncline structures forming a zone are located in the northern Iraq parallel to the Iran border (Figure 2) including main thrust of the Zagros Mountain Belt. The formation is mainly crops out in this folded zone which is called as high folded zone.

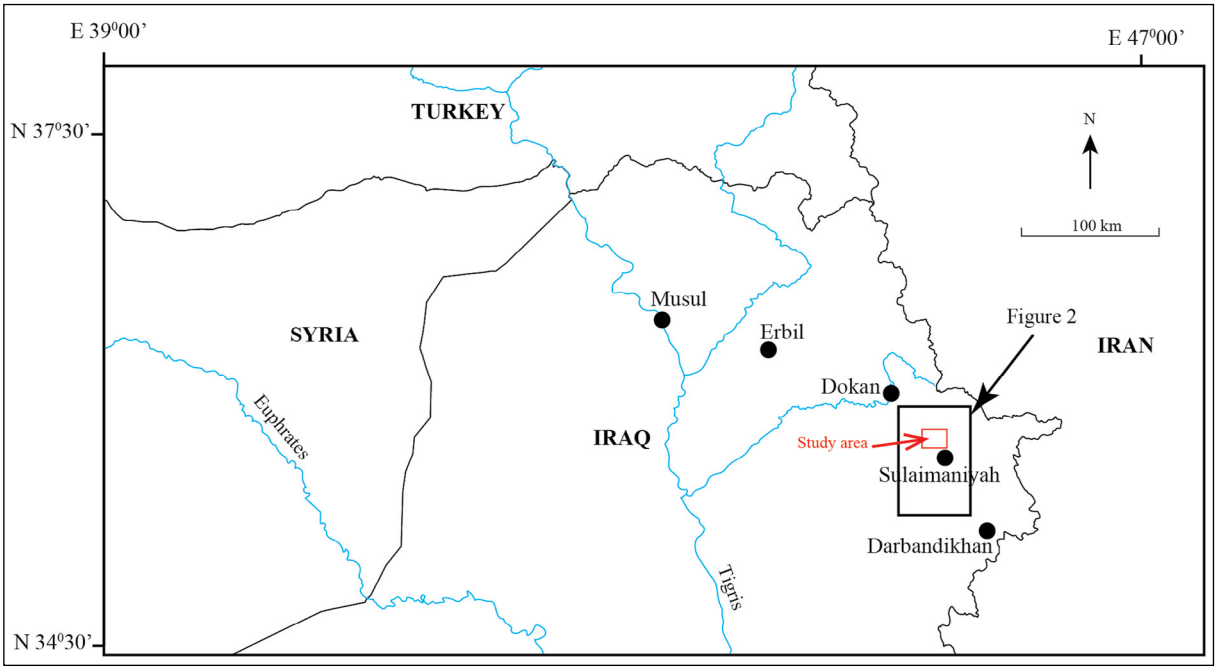

Figure 1- Location map showing study area. Northwestern Sulaimaniyah, northern Iraq.

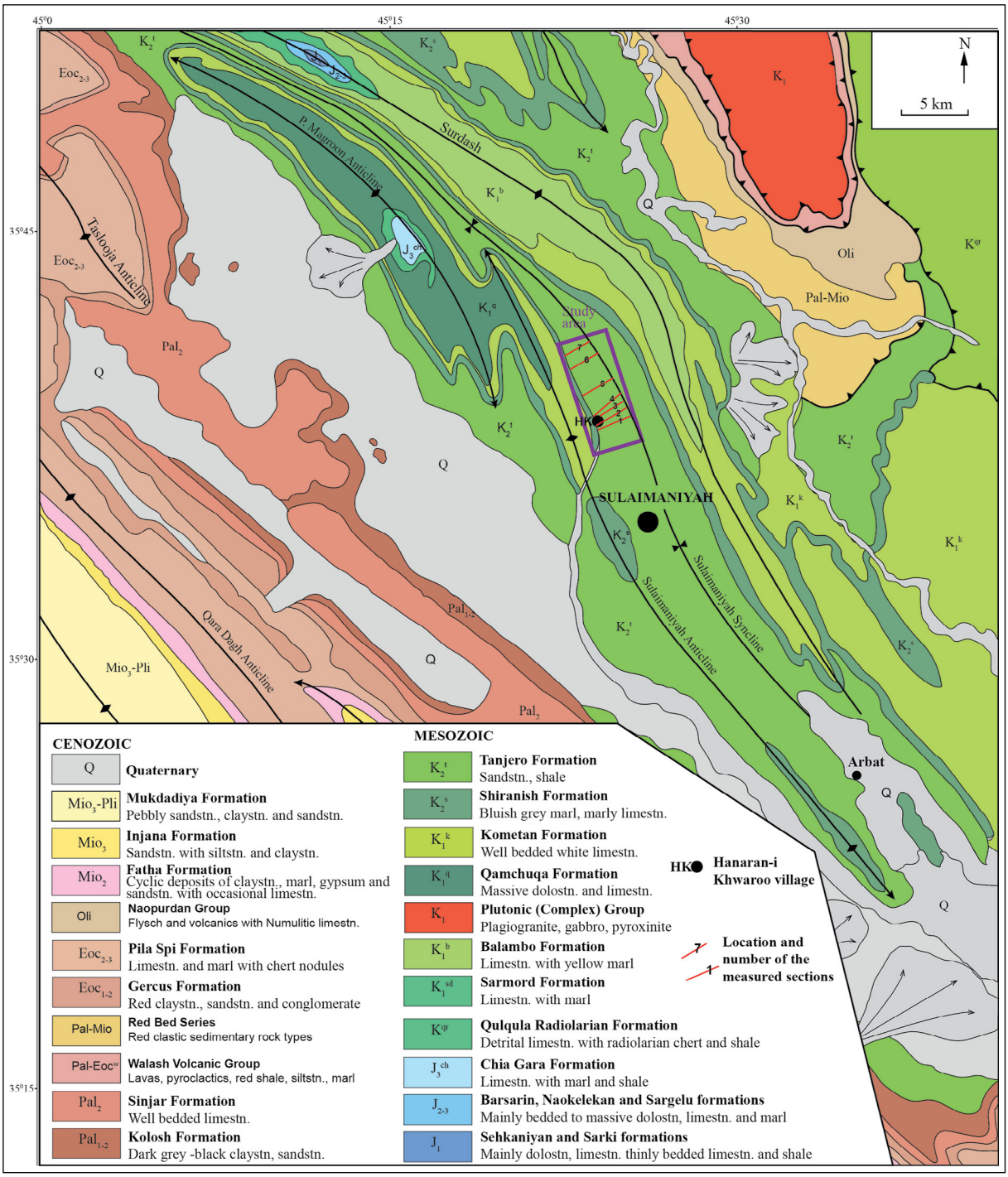

Figure 2- Detailed geological map of the northern Iraq including study area (modified and merged from Sissakian and Fouad, 2015).

The study area is located in the southern limb of the Sulaimaniyah Syncline (Figure 2).

The purpose of this paper is to describe the provenance of the low density turbidite sandstones of Upper Cretaceous Tanjero Formation exposed in the northwestern part of the Sulaimaniyah city, northern Iraq, using palaeoflow and modal analysis in sedimentary petrography. These data are important to determine how the tectonics and geomorphology of the hinterland evolved during Cretaceous.

Modal analysis, and sandstone classification performed for provenance proposes is based on the genetically significant petrographic schemes by Folk (1966), Dickinson and Suczek (1979) and Dickinson

et al. (1983). In the first study (Çelik and Salih, 2018) on the petrographic characteristic and provenance of this formation, it was stated that Lower Cretaceous Balambo and Qamchuqa formations should be found in the feeding area of turbidite sandstones of the Tanjero Formation near Arbat province in northeastern Iraq. Presentpaper, which is a continuation of this study, was applied to the same turbidites cropped out in the northwest of Sulaimaniyah province.In this region, which has not been adequately studied in terms of petrography and therefore has led to incomplete palaeogeographic interpretations, large-scale exposures of this unit along the Iraqi-Iranian border in Darbandikhan (northeastern Iraq) and northwestern part of Sulaimaniyah has also opened a way for studies.

2. Geological Setting

The Tanjero Basin was being located in the northern portion of the Arabian Plate during Late Cretaceous and its deposits cover a wide area along the Iran border in the present day (Figure 2). The geologicalevolution of the basin was controlled by the Late Cretaceous northward subduction of the Arabian plate (Karim, 2004, 2007; Karim et al., 2012, 2014).

The studied area is located south of Zagros Thrust Belt, which is developed from the Neo-Tethys Oceanic basin fill and collision of Iranian and Arabian plates. Structurally the area partly located in the Imbricated and High Folded zones (Buday and Jassim, 1987) which is characterized by anticlines and synclines (Figure 2).

The formation is located at the both limbs of the Sulaimaniyah Syncline (Figure 2) only whereas their continuation along the axis and limb of the anticline is removed by erosion. The northern limit of the outcrop distribution of the unit nearly coincides with the boundary between thrust and imbricated zones.

The stratigraphic units cropped out of the Sulaimaniyah area were summarized in figure 3. In the studied area, Shiranish Formation conformably underlies Tanjero Formation gradationally. The contact is marked at the first appearance of gray sandstone or siltstone beds at the top of Shiranish Formation (bluish white marl and marly limestone) and starting of olive greenish-greyish lithology of Tanjero Formation (Figure 4).

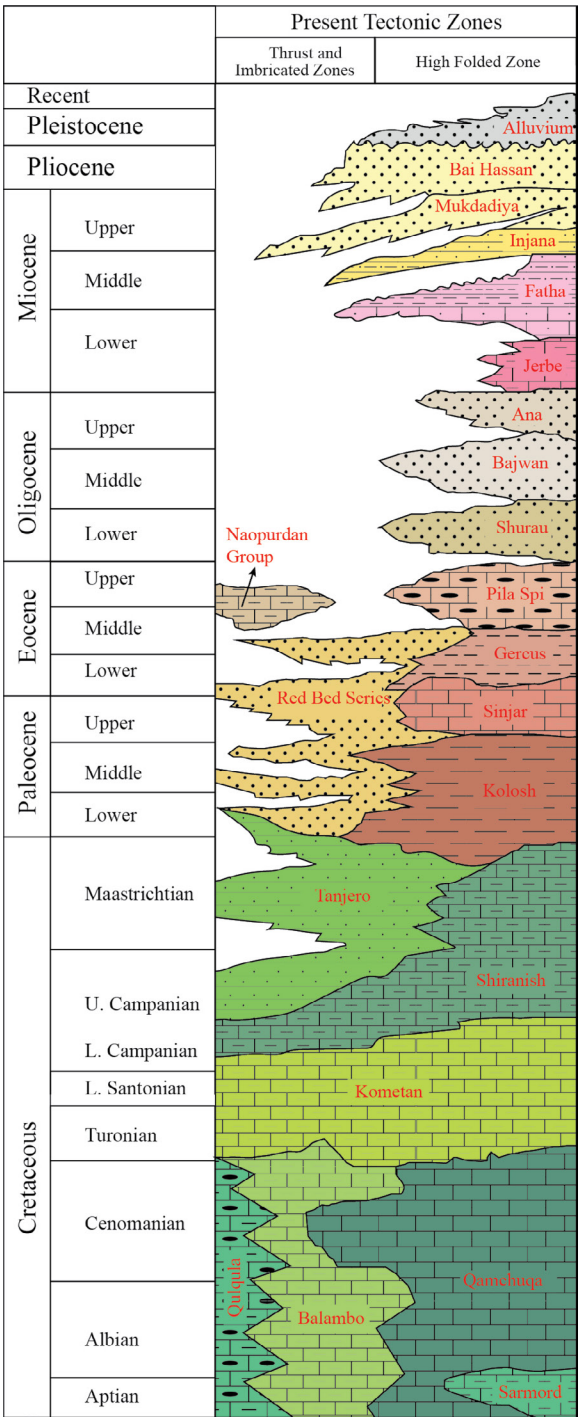

Figure 3- Stratigraphic columnar section of Sulaimaniyah area (no scale), (modified from Karim, 2010).

The unit is characterized by alternation of deep marine low density thin bedded and sheet turbidites (Figure 5 and 6) in the study area on the limbs of the fold andall other outcrops throughout the northern Iraq according to personal field works, despite of the

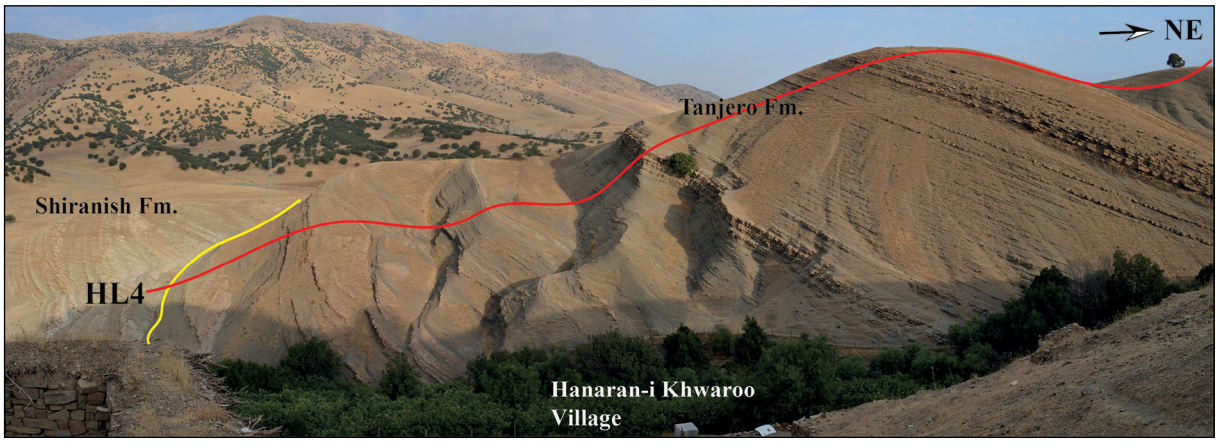

Figure 4- Conformable contact between Shiranish and Tanjero formations. Red line represents line of the measured section 4 (0-96 meters) labelled as HL4. Hanaran-i Khwaroo village, NE of Sulaimaniyah, view to the west (see also figure 2 and figure 8 for location of the village).

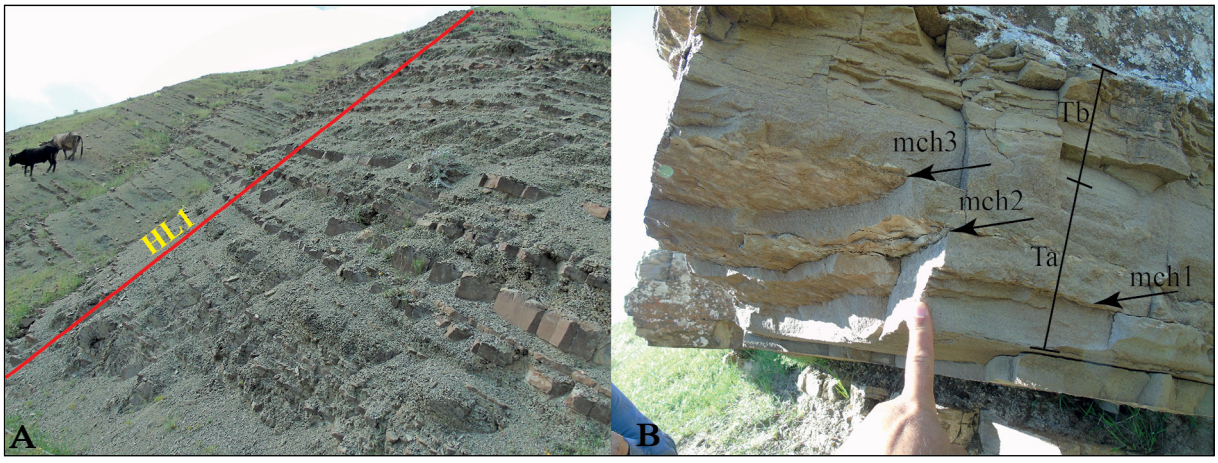

Figure 5- Lobe fringe to lobe distal fringe turbidites of the unit in the HL1 (60-65 meters) (A) and the Ta-b divisions including three mud chip levels (mch1-3) in the normal graded Ta with an erosional base on the underlying finer grained sandstone bed in the 20th meter of HL1 measured section (B). East of the Hanaran-i Khwaroo village, NE of Sulaimaniyah, view to the west.

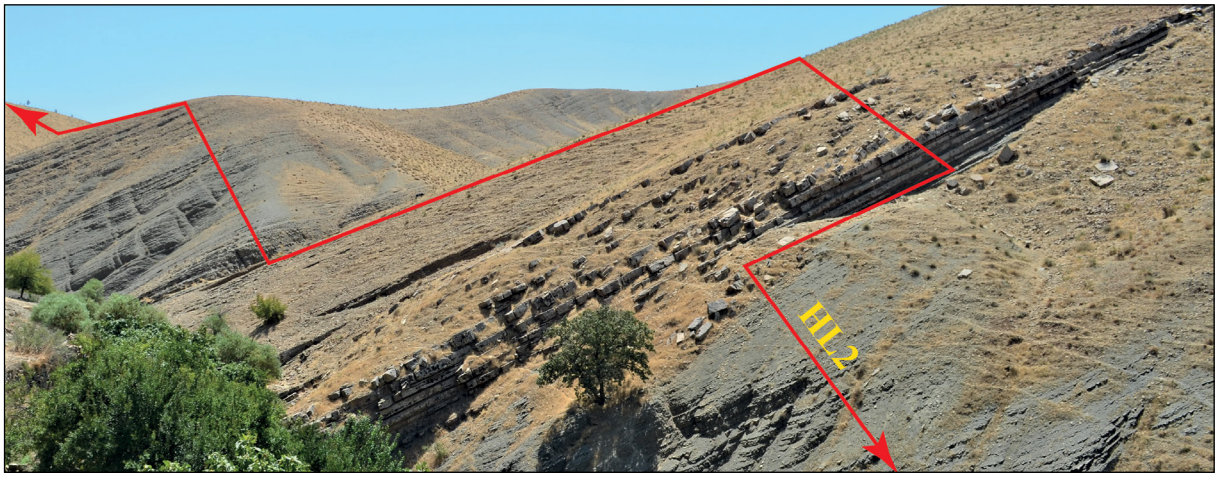

Figure 6- Thin bedded and sheet turbidites of the formation in HL2 (36-72 meters). East of the Hanaran-i Khwaroo village, NE of Sulaimaniyah, view to the east.

previous studies (e.g., Karim, 2004, 2007; Karim et al., 2012) stating conglomerate and limestone alternation outcrops somewhere.

The facies analysis, with the detail seven measured stratigraphic sections (Figure 7) framework including seven distinctive main lithofacies groups and forty-eight subfacies suggest middle part of outer fan and lobe fringe to lobe distal fringe sand rich depositional system in which the sandstone ratio is 18.14 % and shale ratio is 81.86 %. This sandstone/shale ratio (net to gross) is very low and represents distal turbidites.

3. Material and Method

Sixty-nine sandstone samples (labeled as HL1-1 as seen in the figure 7), were collected systematically from seven distinctive measured sections (Figure 8) from superbly exhumed deep marine turbidites of Tanjero Formation in the study area.

Thin section petrographic studies were carried out from 31 samples to identify the mineralogical composition and to apply modal analysis. Compositional analysis (Table 1) and classical point counting method were used to apply the quartz (Q), feldspars (F) and rock fragments (R) ternary diagram of Pettijohn et al. (1987). For each thin section 500 points were counted under a polarized light microscope, following the GD point-counting method (Gazzi, 1966; Dickinson, 1970) in the microscope lab of Geology Department in Fırat University, Turkey.

Palaeoflow data were obtained by following the method of Tucker (2011), from micro-scaled unidirectional and bidirectional sedimentary structures such as flute mark, current ripple, oriented plant materials, parting lineation. These data were statistically processed with the rose diagrams in the software Geo Rose.

Folk's (1951) maturity type table, Folk (1966) Q-F-R ternary diagrams for the classification of the sandstone and Qm-F-Lt provenance ternary diagram of Dickinson et al. (1983) were used in order to differentiate maturity type and major provenance categories.

4. Petrography

A detailed table was formed for petrographic analysis (summarized in Table 1). which includes compositional ratios of Q, F and Rf, cement type, alteration/dissolution, fossils content, sedimentary structures, sorting, roundness, modal classification for Folk's (1966) ternary diagrams, the number of photo taken in each thin section and rock name depended on grain size. The turbidite sandstones are classified as calclithite for the unit according to Folk's (1966) ternary diagrams (Figure 9).

The sandstones are very fine to medium grained (Table 1). Sandstone framework consist of subangular to subrounded rock fragments, very angular lithic cherts and quartz, reworked radiolaria fossils (Figure 10, 11, 12, 13, and 14) with sutured, concavo convex, long grain and little tangential grain contact types (Figure 15, 16, and 17). Poorly sorting (Figure 18) and high compaction ratio increases the grain contact index since the small grains fill the voids between the bigger lithic fragments.

These contact types reflecting the diagenetic events are implying that compaction degree is moderate. The effects of compaction are also manifested in the grain deformation. In the turbidite sandstone studied grains are not deformed, only exhibited evidences of fragile deformation in a few cases, mainly in the grains vertices or within internal grain cracks filled by mainly calcite and solid bitumen (Figure 19, 20 and 21).

Grain contact types and contact index (average number of contacts per grain) supply to researchers the packing character of the sandstone studied. The contact index of the sandstone is 4.7. The contact types of the sandstone in this study point out moderate to tightly packing.

The other grain contact type present in the sandstones of the unit is floating type, which is seen greywacke calclithites since the cement ratio is more than %15, the grains can stay in the calcite cement without having contact with the other fragments in some parts of the thin sections.

Main cement is calcite filling the interstitial pores also replaces the grains, clay and matrix are secondary and in a very low ratio. Solid bitumen fillings are

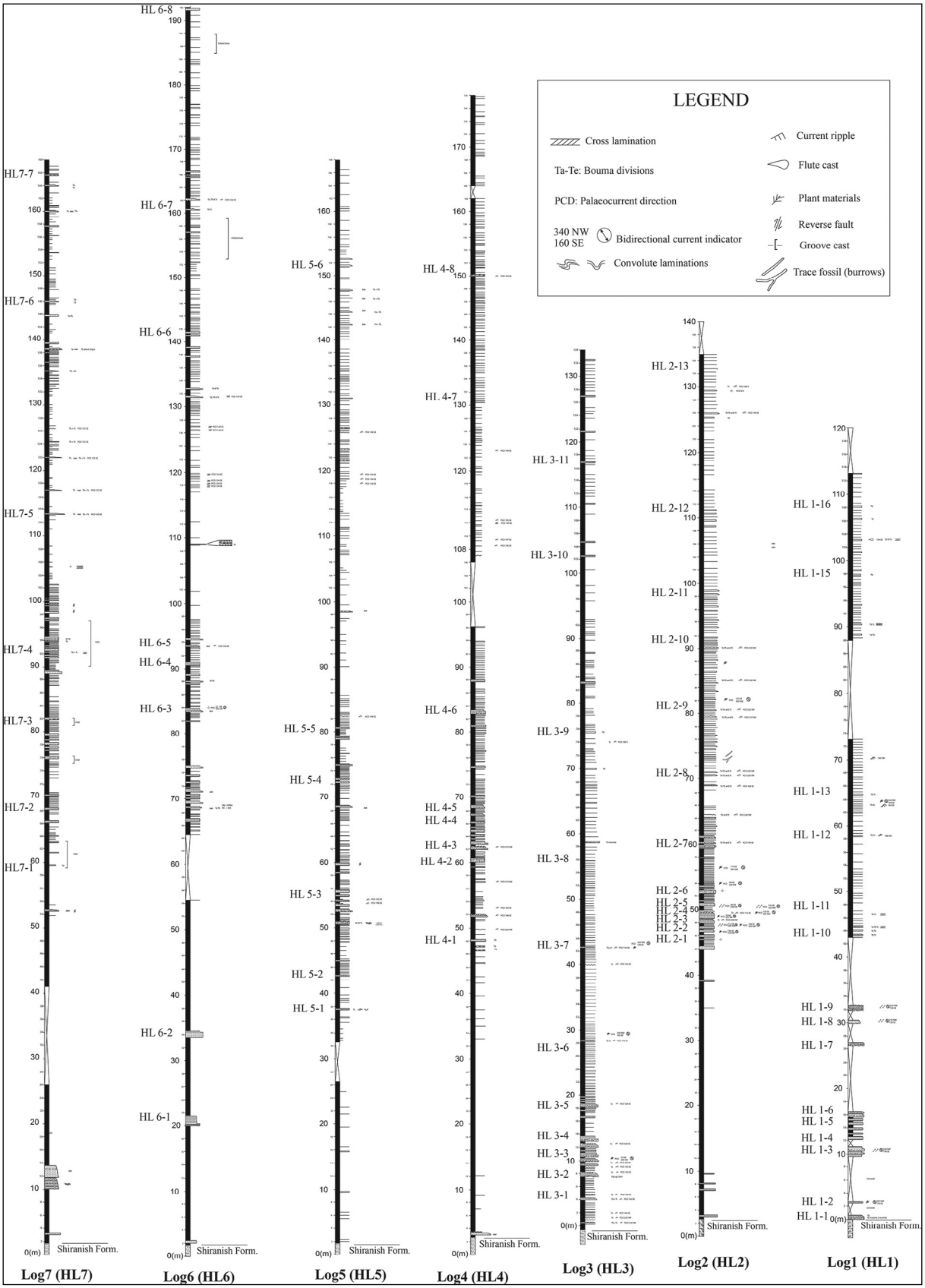

Figure 7- Measured sections logged in the study area. Coordinates of the measured sections (logs) are: HL1: N 35040’14.10’’ E 45022’38.39’’, HL2: N 35040’23.27’’ E 45022’35.79’’, HL3: N 35040’30.46’’ E 45022’38.18’’, HL4: N 35040’28.23’’ E 45022’30.06’’, HL5: N 35040’58.51’’ E 45022’11.78’’, HL6: N 35041’31.06’’ E 45021’36.80’’, HL7: N 35041’56.19’’ E 45021’19.54’’,

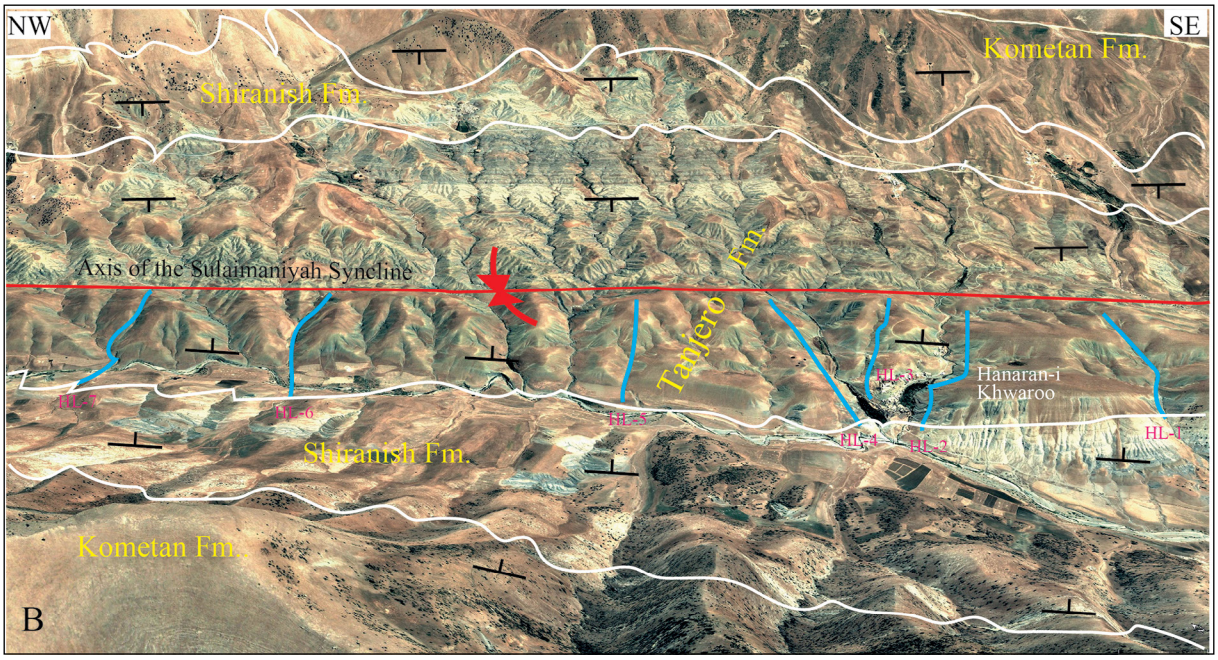

Figure 8- Google Earth image covering the study area around the Hanaran-i Khwaroo village located just where the HL-3 starts, northeast of Sulaimaniyah. Formations are repeating because of the Sulaimaniyah Syncline axis located approximately in NW-SE orientation where the logs end (see also Figure 2). For the scale, the thickness of HL1 is 120m. See Figure 7 for thickness of the other measured sections. View to the northeast.

seen in many thin section (Table 1, in the "other components" column) and it blocks pore spaces and stain the calcite cement to brownish – yellowish in colour which present in the all microphotographs except figure 15.

The only quartz type from the source area in the turbidite sandstone is monocrystalline, very angular to angular with straight fully extinction common quartz (see Figure 13, 14 and 15). The ratio of the quartz is 0.37% in average (Table 1) for the unit in this study.

Rare heavy mineral presence is notable with low concentration. Hematite and euhedral to subhedral black opaque minerals (were not differentiated in this study) are the most common. Feldspar ratio is 0,009% for the whole sandstone samples. It was seen with highly alteration in one sample (Table 1 with 0.3 percentages).

Carbonate rock fragments are the main lithoclasts constituent of the turbidite sandstone with 59.32 percentages. Chert without radiolaria has 16.65 percentages and the others are shale, silt, released-reworked radiolaria fossils, benthic fossil shell fragments, glauconite, radiolarian chert and radiolarian mudstone fragments with a ratio of 24.03% (Table 1). No any metamorphic or magmatic rock clast was seen in the sandstone thin sections.

All the petrographic examines show that the turbidite sandstones of Upper Cretaceous Tanjero Formation, having less than 5 percentage clay, angular to subangular grains, poorly sorting, dominant tangential and point, a few sutured contact types, are submature (Figure 22).

Submature stage for the sandstones implies a short distance transportation of the lithic clasts into the deep marine environment of the Upper Cretaceous basin.

5. Provenance

Petrographic data obtained from the thin sections were applied to the Qm-F-Lt ternary diagram of Dickinson et al. (1983) to interpret the tectonic provenance of the sandstones. The modal classification indicates that the sedimentary rocks are included within the "lithic recycled" category (Figure 23). Also palaeoflow rose diagrams (Figure 24 and Figure 25) from the unidirectional and bidirectional sedimentary structures in the turbidites, indicate SE direction which useful to accurately establish the location of source area.

Table 1- Petrographic content of the thin sections (the numbers for Q, F and RF were rounded to the nearest whole numbers).

No	Thin Section No:	%Q	%F	%RF	Cement	Matrix	Other components	Alteration/ dissolution	Fossils	Sedimentary structures	Sorting	Roundness	Modal Classification	No. of photos	Rock name
1	HL 1-1	1	-	99 (chrt:8,Crbnt:65, Mudstone +released radiolaria:27)	Calcite	-	Bitumen fillings + euhedral to subhedral opaque minerals	Carbonate rock clasts to calcite	Fossil shell fragments+ reworked radiolaria	Slightly pebble orientation	Moderately	Subangular rock clasts, very angular cherts and quartz	Calclithite	6	Very fine grained sandstone
2	HL 1-2	1,6	-	98,4 (chrt:27,Crbnt:55, Mudstone +released radolaria:18)	Calcite	-	Bitumen fillings + euhedral to subhedral opaque minerals	Carbonate rock clasts to calcite	Fossil shell fragments+ reworked radiolaria	Slightly pebble orientation	Moderately	Subangular rock fragments, very angular cherts and quartz	Calclithite	6	Very fine grained sandstone
3	HL 1-7	0,4	-	99,6 (chrt:25,Crbnt:60, mudstone with and/ released radiolaria:15)	Calcite	-	Bitumen fillings + euhedral to subhedral opaque minerals+ carbonized plant materials	Carbonate rock clasts to calcite	Fossil shell fragments+ reworked radiolaria	Slightly pebble orientation	Moderately	Subangular-subrounded rock fragments, very angular cherts and quartz	Calclithite	6	Very fine grained sandstone
4	HL1-8	0,5	-	99,5 (chrt:27,Crbnt:53, mudstone with and/ released radiolaria:20)	Calcite	-	Bitumen fillings + euhedral to subhedral opaque minerals	Carbonate rock clasts to calcite	Fossil shell fragments+ reworked radiolaria	Slightly pebble orientation	Poorly	Subrounded rock fragments, very angular cherts and quartz	Calclithite	4	Very fine grained sandstone
5	HL1-9	0,3	-	99,7 (chrt:19, Crbnt:58, Siltstone, mudstone with and/ released radiolaria and others:23)	Calcite	-	Glauconite+ bitumen fillings + euhedral to subhedral opaque minerals	Carbonate rock fragments to calcite	Rare benthic shell fragments+ plenty of reworked radiolaria	-	Very poorly	Subangular rock fragments, very angular cherts and quartz	Calclithite	14	Pebbly fine grained sandstone
6	HL1-14	1	-	99 (chrt:10, Crbnt:50, Siltstone, mudstone with and/ released radiolaria and others:40)	Calcite	-	Bitumen fillings + carbonized plant materials	Carbonate rock fragments to calcite	Reworked radiolaria	-	Poorly	Subangular-subrounded rock fragments, very angular cherts	Calclithite	10	Pebbly fine grained sandstone

Table 1- (continue).

No	Thin Section No:	%Q	%F	%RF	Cement	Matrix	Other components	Alteration/ dissolution	Fossils	Sedimentary structures	Sorting	Roundness	Modal Classification	No. of photos	Rock name
7	HL 2-3	1	0,3	98,7 (chrt:10,Crbnt:55, Mudstone with and / released radiolaria and others:35)	Calcite	-	Bitumen fillings + euhedral to subhedral opaque minerals	Feldspar to clay+ Carbonate rock fragments to calcite	Rare benthic shell fragments+ reworked radiolaria	Wavy deformed secondary calcite in fractures	Moderately	Subrounded rock fragments, very angular cherts and quartz	Calclithite greywacke	8	Pebbly fine grain sandstone
8	HL 2-4	0,3	-	99,7 (chrt:33, Crbnt:46, Siltstone, mudstone with and/ released radiolaria and others:21)	Calcite	-	Glauconite+ Bitumen fillings + euhedral to subhedral opaque minerals	Carbonate rock fragments to calcite	Globigerina +benthic shell fragments+ reworked radiolaria	Grain orientation throughout the section	Very poorly	Subangular rock fragments, very angular cherts and quartz	Calclithite	20	Medium grained sandstone
9	HL 2-7	-	-	100 (chrt:10,Crbnt:60, Siltstone, mudstone with and/ released radiolaria and others:30)	Calcite	-	Opaque angular heavy minerals 2%+ glauconite (0,2 %) +plant materials and pellets (0,3%)	Carbonate rock fragments to calcite	Reworked radiolaria	-	Poorly	Subangular-subrounded rock fragments, very angular cherts	Calclithite	2	Very fine grained sandstone
10	HL2-10	-	-	100 (chrt:10,Crbnt:65, Siltstone, mudstone with and/ released radiolaria and others:25)	Calcite	-	Bitumen fillings	?	Rare benthic shell fragments+ reworked radiolaria	-	Poorly	Subangular-subrounded rock fragments, very angular cherts	Calclithite	6	Very fine grained sandstone
11	HL2-13	0,5	-	99,5 (chrt:17,Crbnt:37, Siltstone, mudstone with and/ released radiolaria and others:46)	Calcite	+	Opaque angular heavy minerals 1%+ bitumen fillings	Carbonate rock fragments to calcite	Reworked radiolaria	-	Poorly		Calclithite	6	Fine grained sandstone
12	HL 3-2	-	-	100 (chrt:30 ,Crbnt:50, Siltstone, mudstone with and/ released radiolaria and others:20)	Calcite	-	Very well rounded glauconite + carbonized plant materials+ bitumen fillings	Carbonate rock fragments to calcite	Reworked radiolaria and fossil shell fragments	Compaction and contact types	Poorly	Subangular-subrounded rock fragments, very angular cherts	Calclithite	24	Pebbly fine grained sandstone

Table 1- (continue).

No	Thin Section No:	%Q	%F	%RF	Cement	Matrix	Other components	Alteration/ dissolution	Fossils	Sedimentary structures	Sorting	Roundness	Modal Classification	No. of photos	Rock name
13	HL 3-4	-	-	100 (chrt:26, Crbnt:54, Siltstone, mudstone with and/ released radiolaria and others:20)	Calcite	-	Very well rounded glauconite + carbonized plant materials+ bitumen fillings	Carbonate rock fragments to calcite	Reworked radiolaria and fossil shell fragments	Compaction and contact types	Poorly	Subangular-subrounded rock fragments, very angular cherts	Calclithite	-	Pebbly fine grained sandstone
14	HL 3-6	-	-	100 (chrt:5,Crbnt:80, Mudstone with radiolaria+ released radiolaria:15)	Calcite	-	Bitumen fillings	Carbonate rock fragments to calcite	Reworked radiolaria + globigerina	grain orientation makes lineation in the section	Moderately	Subangular-subrounded rock fragments, angular cherts	Calclithite	2	Very fine grained sandstone
15	HL3-11	0,5	-	99,5 (chrt:5, Crbnt:75, Siltstone, mudstone with and/ released radiolaria and coal fragments:20)	Calcite	-	Opaque euhedral heavy minerals 1%+ glauconite+ bitumen fillings+ carbonized plant materials	Carbonate rock fragments to calcite	Fossil shell fragments+ reworked radiolaria	-	Poorly	Subangular-subrounded rock fragments and quartz very angular cherts	Calclithite	37	Fine grained sandstone
16	HL 4-1	1	-	99 (chrt:11, Crbnt:62, Siltstone, mudstone with and/ released radiolaria and others:27)	Calcite	-	Opaque euhedral heavy minerals 1,5%+ glauconite+ bitumen fillings+ carbonized plant materials	Carbonate rock fragments to calcite	Fossil shell fragments+ reworked radiolaria	grain orientation makes lineation in the section	Poorly	Subangular-subrounded rock fragments, very angular cherts and quartz	Calclithite	6	Very fine grained sandstone
17	HL 4-2	0,8	-	99,8 (chrt:32,Crbnt:40, Siltstone, mudstone with and/ released radiolaria and others:28)	Calcite	-	-	Carbonate rock fragments to calcite	Reworked radiolaria	-	Poorly	subrounded rock fragments, very angular cherts and quartz	Calclithite	8	Very fine grained sandstone
18	HL 4-3	-	-	100 (chrt:4,Crbnt:74, Siltstone, mudstone with and/ released radiolaria and others:22)	Calcite	-	-	Carbonate rock fragments to calcite	Reworked radiolaria	-	Moderately	subrounded rock fragments, very angular cherts	Calclithite	2	Very fine grained sandstone

Table 1- (continue).

No	Thin Section No:	%Q	%F	%RF	Cement	Matrix	Other components	Alteration/ dissolution	Fossils	Sedimentary structures	Sorting	Roundness	Modal Classification	No. of photos	Rock name
19	HL 4-5	0,2	-	99,8 (chrt:9, crbnt:77, siltstone, mudstone with and/ released radiolaria and others:14)	Calcite about %25	-	Opaque subhedral heavy minerals + glauconite + bright reddish hematite+ rare tiny bitumen fillings	Carbonate rock fragments to calcite	Rare benthic shell fragments+ reworked radiolaria + 2 globigerina	-	Moderately	Subangular- rock fragments, very angular cherts and quartz	Calclithite (greywacke)	7	Fine grained sandstone
20	HL 4-6	0,2	-	99,8 (chrt:14, crbnt:72, siltstone, mudstone with and/ released radiolaria and others:14)	Calcite about %25	-	Opaque subhedral heavy minerals + glauconite + bright reddish hematite+ tiny bitumen fillings	Carbonate rock fragments to calcite	Rare benthic shell fragments+ reworked radiolaria	-	Poorly	Subangular- rock fragments, very angular and needle shaped cherts and angular quartz	Calclithite (greywacke)	10	Fine grained sandstone
21	HL4-7	-	-	100 (chrt:27,Crbnt:55, Siltstone, mudstone with and/ released radiolaria and others:18)	Calcite	-	Opaque subhedral heavy minerals + plant materials+ glauconite + bright reddish hematite+ rare bitumen fillings	Carbonate rock fragments to calcite	Rare benthic shell fragments+ reworked radiolaria	-	Very poorly	Subangular-subrounded rock fragments, very angular cherts	Calclithite	8	Fine grained sandstone
22	HL4-8	-	-	100 (chrt:27,Crbnt:55, Siltstone, mudstone with and/ released radiolaria and others:18)	Calcite	-	Opaque subhedral heavy minerals+ bitumen fillings	Carbonate rock fragments to calcite	Rare benthic shell fragments+ reworked radiolaria	-	Very poorly	Subangular-subrounded rock fragments, very angular cherts	Calclithite	10	Very fine grained sandstone
23	HL 5-2	0,5	-	99,5 (chrt:20,Crbnt:45, Siltstone, mudstone with and/ released radiolaria and others:35)	Calcite	-	Subangular glauconite + black subhedral heavy minerals + bitumen fillings	Carbonate rock fragments to calcite	Rare benthic shell fragments+ reworked radiolaria	Slightly grain orientation	Very poorly	Subangular-subrounded rock fragments, very angular cherts	Calclithite	10	Very fine grained sandstone

Table 1- (continue).

No	Thin Section No:	%Q	%F	%RF	Cement	Matrix	Other components	Alteration/ dissolution	Fossils	Sedimentary structures	Sorting	Roundness	Modal Classification	No. of photos	Rock name
24	HL 5-3	0,4	-	99,6 (chrt:6,Crbnt:72, Siltstone, mudstone with and/ released radiolaria and others:22)	Calcite	-	Subangular glauconite + bitumen fillings	Carbonate rock fragments to calcite	Rare benthic shell fragments+ reworked radiolaria	Slightly grain orientation	Poorly	Subangular-subrounded rock fragments, very angular cherts and quartz	Calclithite	4	Very fine grained sandstone
25	HL 5-4	0,2	-	99,8 (chrt:23,Crbnt:47, Siltstone, mudstone with and/ released radiolaria and others:30)	Calcite	-	Rare bitumen fillings + glauconite	Carbonate rock fragments to calcite	Rare benthic shell fragments+ plenty of reworked radiolaria	-	Poorly	Subangular rock fragments, very angular cherts and quartz	Calclithite	10	Very fine grained sandstone
26	HL 6-3	0,5	-	99,5 (chrt:22,Crbnt:54, Siltstone, mudstone with and/ released radiolaria and others:34)	Calcite	-	Bitumen fillings	Carbonate rock fragments to calcite	Rare benthic shell fragments+ plenty of reworked radiolaria	Slightly grain orientation	Very poorly	Subangular-subrounded rock fragments, very angular cherts	Calclithite	4	Very fine grained sandstone
27	HL 6-5	-	-	100 (chrt:21,Crbnt:59, Siltstone, mudstone with and/ released radiolaria and others:20)	Calcite	-	Opaque subhedral heavy minerals +bitumen fillings	Carbonate rock fragments to calcite	Rare benthic shell fragments+ plenty of reworked radiolaria	Slightly grain orientation	Poorly	Subangular-subrounded rock fragments, very angular cherts	Calclithite	6	Fine grain siltstone
28	HL 6-7	0,2	-	99,8 (chrt:9, Crbnt:64, Siltstone, mudstone with and/ released radiolaria and others:27)	Calcite	-	Pretty much bitumen fillings+ glauconite	Carbonate rock fragments to calcite	Rare benthic shell fragments+ plenty of reworked radiolaria	Slightly grain orientation in some part of the section	Poorly	Subangular-subrounded rock fragments, very angular cherts and quartz	Calclithite	14	Fine grained sandstone

Table 1- (continue).

No	Thin Section No:	%Q	%F	%RF	Cement	Matrix	Other components	Alteration/ dissolution	Fossils	Sedimentary structures	Sorting	Roundness	Modal Classification	No. of photos	Rock name
29	HL 7-3	0,4	-	99,6 (chrt:7, Crbnt:82, Siltstone, mudstone with and/ released radiolaria and others:11)	Calcite (%25)	-	Glauconite + hematite + rare bitumen fillings	Carbonate rock fragments to calcite	Rare benthic shell fragments+ plenty of reworked radiolaria	Slightly grain orientation and dark lithics form lamina like levels along the section	Moderately	Subangular-subrounded rock fragments, very angular cherts and quartz	Calclithite (greywacke)	7	Very fine grained sandstone
30	HL7-4	-	-	100 (chrt:17,Crbnt:56, Siltstone, mudstone with and/ released radiolaria and others:27)	Calcite	-	Subangular glauconite black subhedral heavy minerals + bitumen fillings	Carbonate rock fragments to calcite	Rare benthic shell fragments+ plenty of reworked radiolaria	Slightly grain orientation	Poorly	Subangular-subrounded rock fragments, very angular cherts	Calclithite	6	Very fine grained sandstone
31	HL7-7	-	-	100 (chrt:15,Crbnt:62, Siltstone, mudstone with and/ released radiolaria and others:23)	Calcite	+	?	Carbonate rock fragments to calcite	Rare benthic shell fragments (0,2%)+plenty of reworked radiolaria	-	Very poorly	Subangular-subrounded rock fragments, very angular cherts	Calclithite	20	Fine grained sandstone
Average		0,37	0,009	Lithic chert : 16,65 Carbonate rf : 59,32 Others :24,03	Calcite	-	Carbonized plant fragments, euhedral to subhedral opaque minerals, reddish brownish hematite, bright green subrounded glauconite, solid bitumen fillings (range between 1-15%) in pores	Carbonate rock fragments to calcite	Globigerina, reworked radiolaria, neritic fossil shell fragments	Slightly grain orientation (not represent-ative for the all sections)	Very poorly to modera-tely	Subangular-subrounded rock fragments, very angular cherts and quartz	Calclithite	9,4333	Very fine to medium grained sandstone

Note: All the quartzs in the thin sections are monocrystalline with straight and fully extinction.

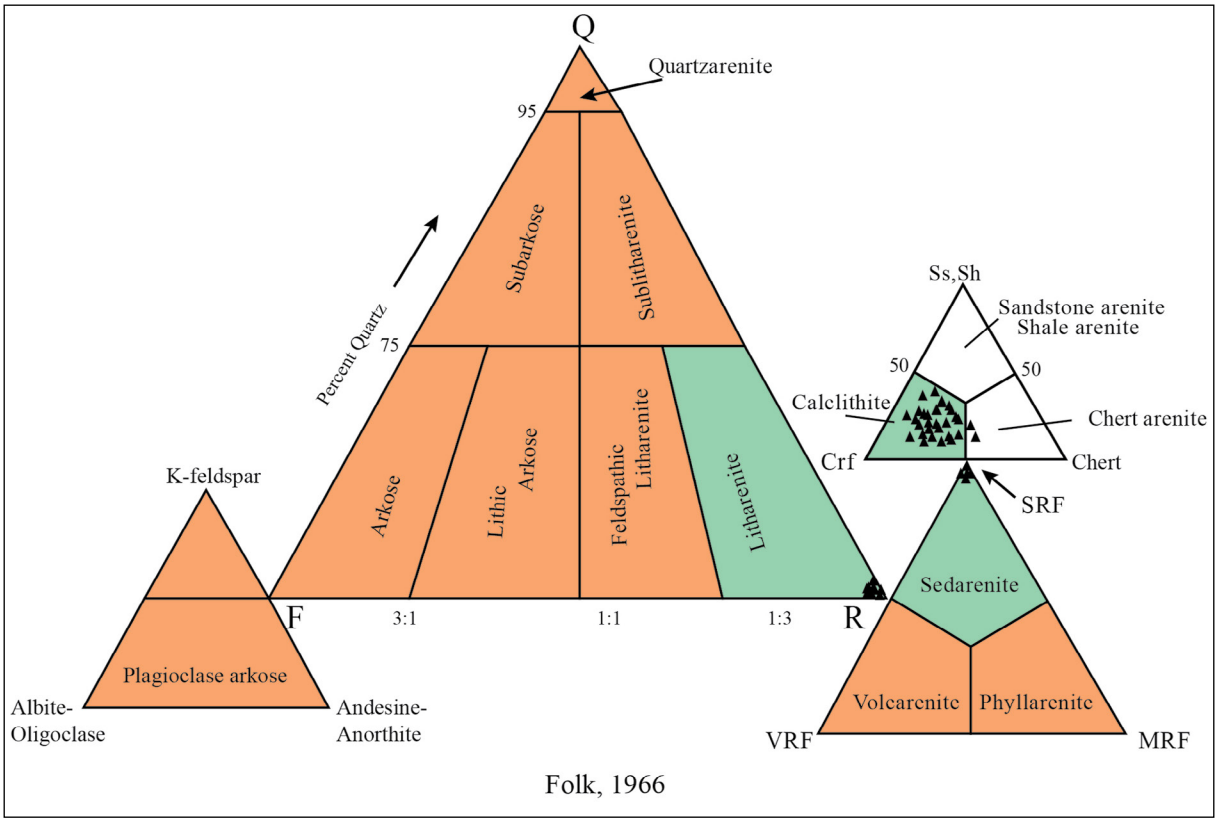

Figure 9- Q-F-R ternary diagrams (Folk, 1966) showing the classification of the turbidite sandstone studied. All the samples fall in the calclithite corner.

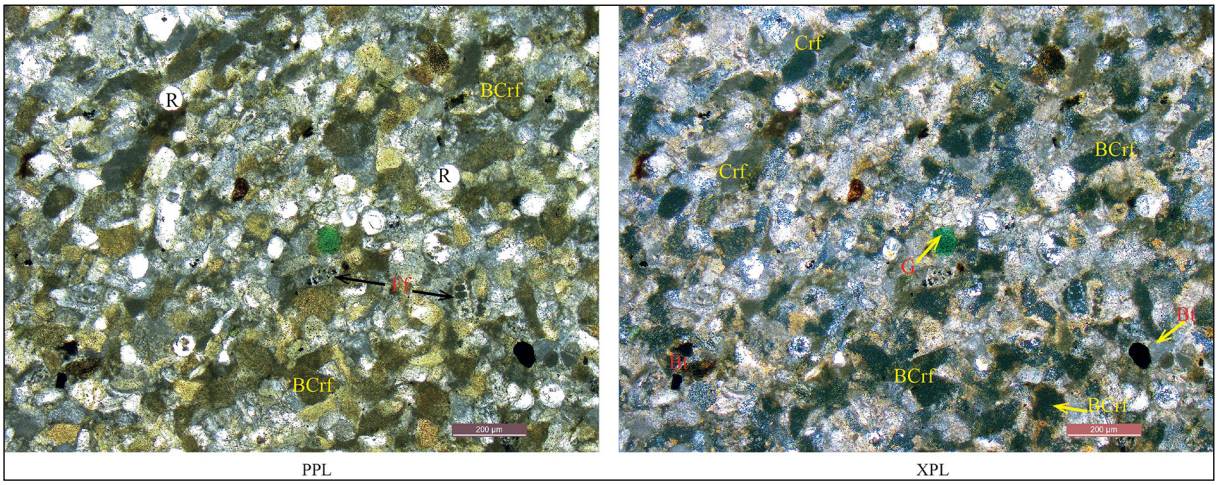

Figure 10- HL1-1. These two photomicrographs (4X-Magnification) represent general composition of the turbidites studied of Tanjero Formation. As the scale is very small it is not possible labelling all the clasts in the images. Dark dirty yellowish to brownish (PPL) angular to subangular clasts are BCrf as labeled some of them. Bluish angular fragments (XPL), angular white fragments (PPL) are lithic chert clasts. Solid bitumen (Bt) fillings are staining the calcite cement to yellowish- brownish in colour. White circles (PPL) are released-reworked radiolaria fossils. Rounded glauconite grain (G) is from shallow water environment. Two neritic fossil shell (Ef) clasts (reworked) are seen here which very rare in the all thin sections. More detail explanations will be in the following photo micrographs.

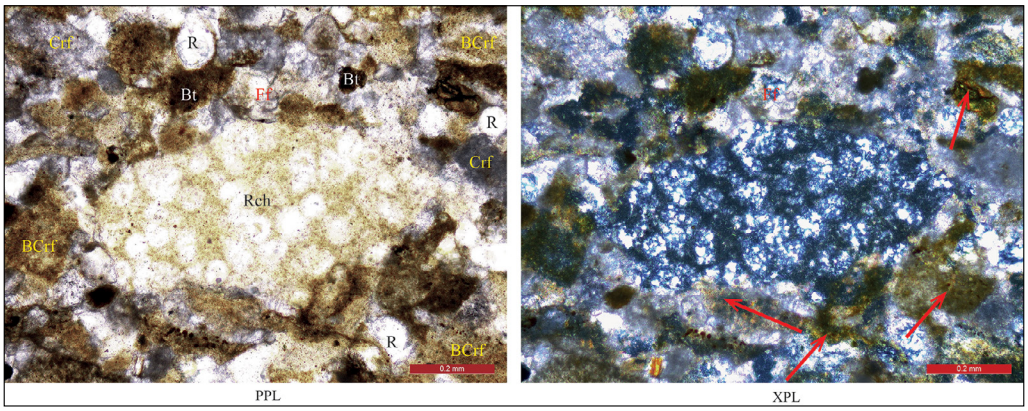

Figure 11- HL1-7. A big radiolaria fossils (white circular specks in Rch in PPL image) bearing angular radiolarian lithic chert clast (Rch). This is the host rock for released and reworked radiolaria fossils in the source area. The released fossils possibly left the host rock either during weathering or transportation. Red arrows point out the bitumen stained calcite cement. Very poorly sorted example for the sandstone studied.

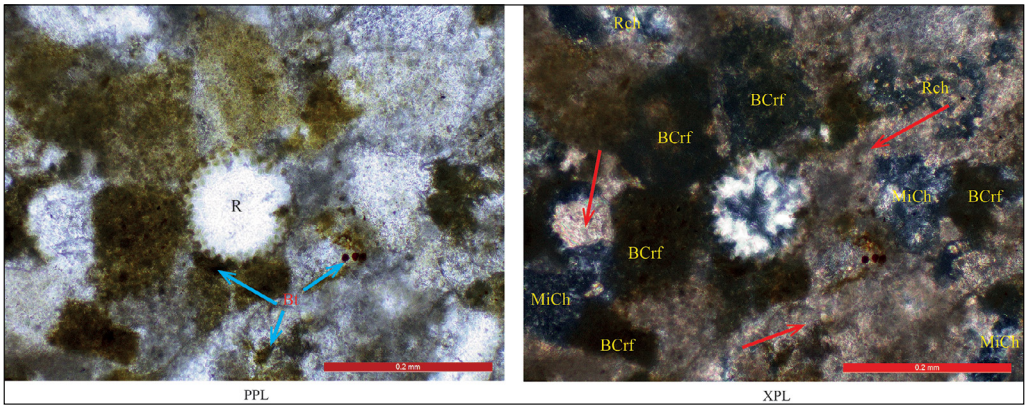

Figure 12- HL1-7. Released and reworked chalcedony filled (XPL view) radiolaria fossil in the center of the image. Although weathering and transportation, the forms of the fossil were nearly well sheltered. Note the concavo convex contact type (the best view PPL image) between the R and the surrounding BCrf fragments. Disseminated (black small circles) solid bitumen fillings are shown by the blue arrows directed to the right up hand side. Bitumen stained calcite cement is represented by red arrows in the XPL image. Mostly all the clasts (especially Rch) were replaced by calcite so the contact of the clast are not very clear in (XPL).

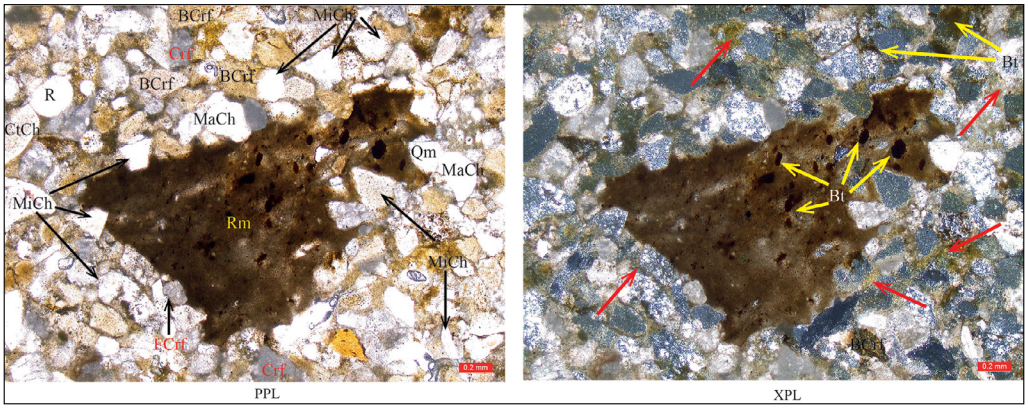

Figure 13- HL1-9. About 2 mm in size radiolarian mudstone clast including chert clasts and solid bitumen fillings. Good example for concavo convex grain contact type since the partly embedding of the all other lithic clasts into the mudstone along the contact. The Rm is most likely was a relatively softer mud intraclast during compaction than the other constituents transported from the source area. Tangential, point and long grain contact types are also present in the images (more visible in the PPL) Solid bitumen fillings in some pores caused the changing of the colour of calcite cement to greenish-yellowish. Very poorly sorted very angular cherts and subangular- subrounded carbonate rock fragments.

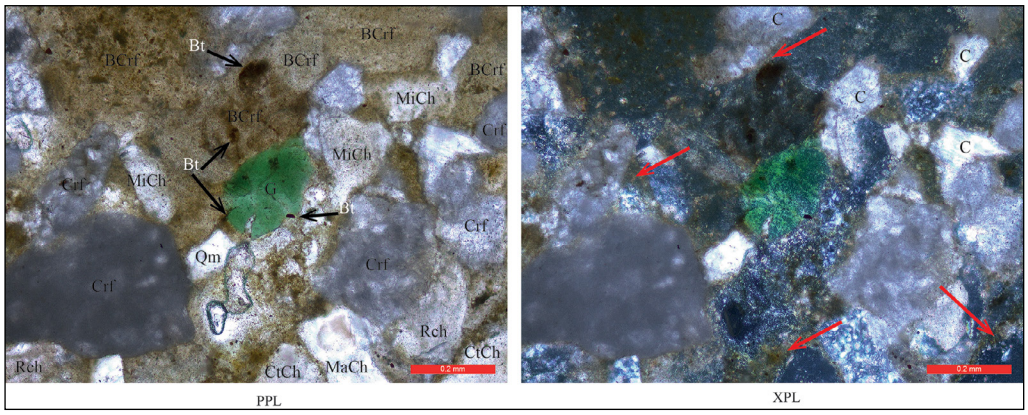

Figure 14- HL1-9. Well rounded reworked bright green glauconite has calcite and bitumen intrusion into the lower part through a small fracture occurred before settling. Two air bubbles as section fault below G. Crf clasts have undefined microfossils as white speckles. Sutured contact type visible between Rch and Crf above the scale bar (PPL), concavo convex contact type between G and two BCrf above G, point contact type between big Crf and the two clasts above (PPL). Calcite cement around the clasts was stained as dark brownish-greenish-yellowish in colour by bitumen fillings.

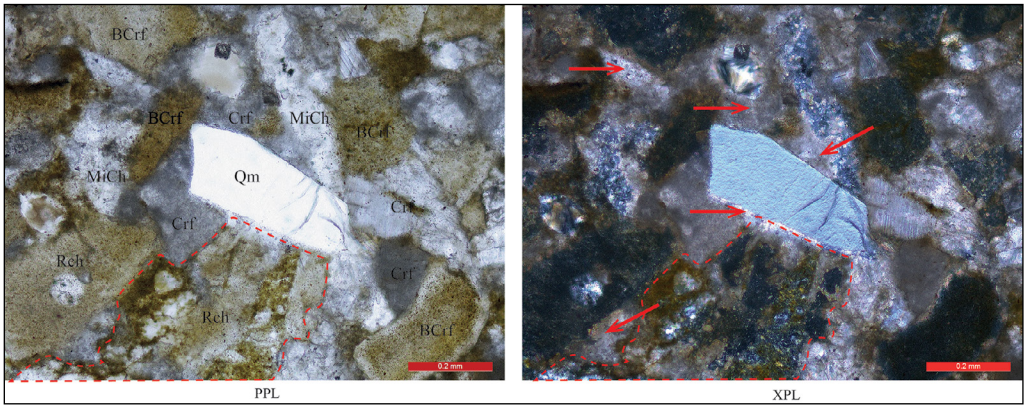

Figure 15- HL1-9. A superb example for very angular monocrystalline quartz (Qm) having straight full extinction in the center of the images. It has a very less ratio in the all thin sections. The Qm inserted into the Crf to the left hand side and split the Crf into two parts during compaction. Long grain contact between the majority of the lithic clasts indicate a tight packing and strong compaction. A big Rch grain located in the lower part of the photo mostly was replaced by calcite (bitumen stained, although Bt is not in this image but exist in the thin section HL1-9).

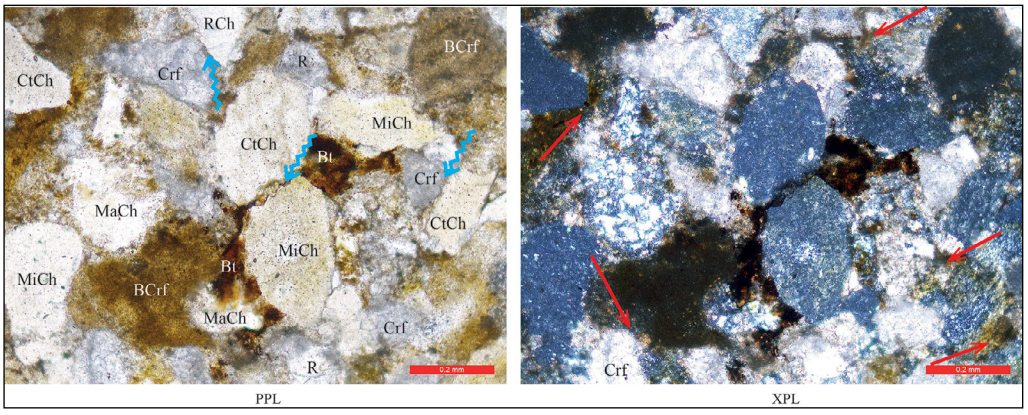

Figure 16- HL2-4. Concavo convex and sutured grain contact types are important for this section. Two Mach grains have concavo convex contact with the dark BCrf clast in the lower left part of the center of the image. Blue arrows indicate the sutured grain contacts. Solid bitumen filling which one of the most effective agents reducing porosity of the sandstones is blocking the intergranular pores and stains the calcite cement.

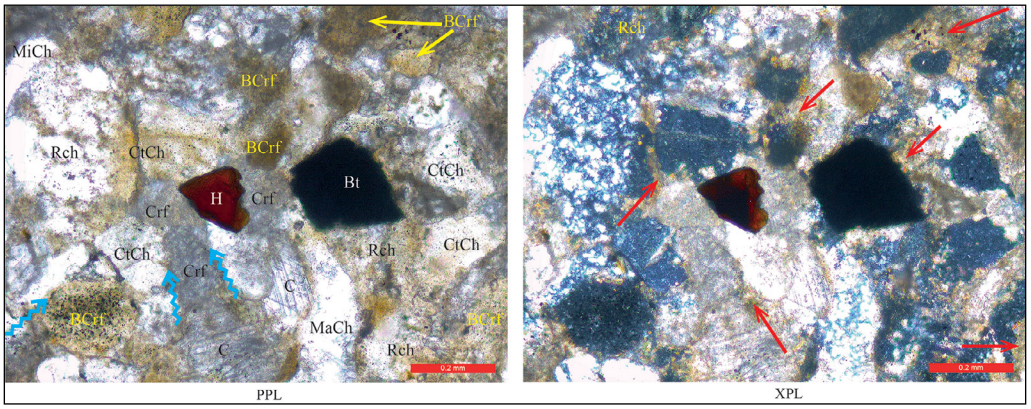

Figure 17- HL4-2. Solid bitumen filling in an intergranular pore and brownish red hematite in the middle part of the photomicrograph. Tightly compaction and sutured grain contact show the high compaction ratio. Rhc clasts were mostly replaced by calcite.

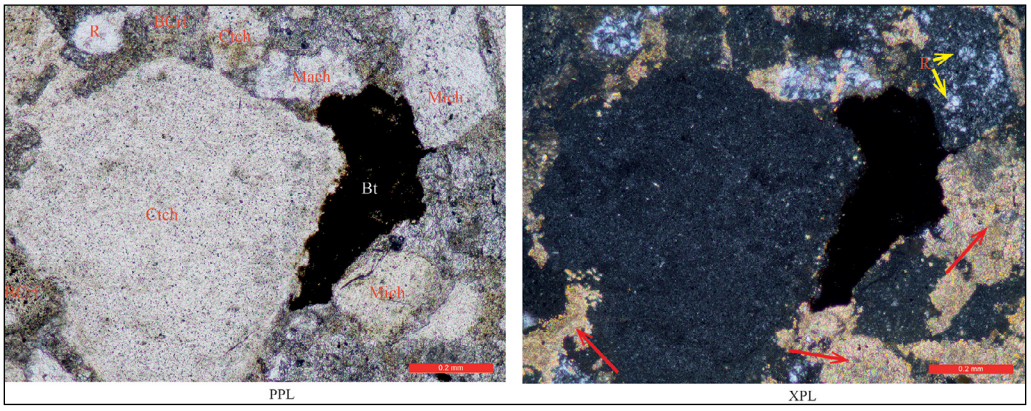

Figure 18- HL4-7. Macrocrystalline microcrystalline and cyrptocrystalline lithic chert clasts are seen together in one image. Red arrows represent slightly stained calcite cement. Solid bitumen visible in both images causes pale yellowish staining on the calcite cement. Note the point contact type between the big CtCh clast and two small lithic chert fragments above. Mich below bitumen filling has floating contact type as it is surrounded by fillings (Calcite cement and Bt).

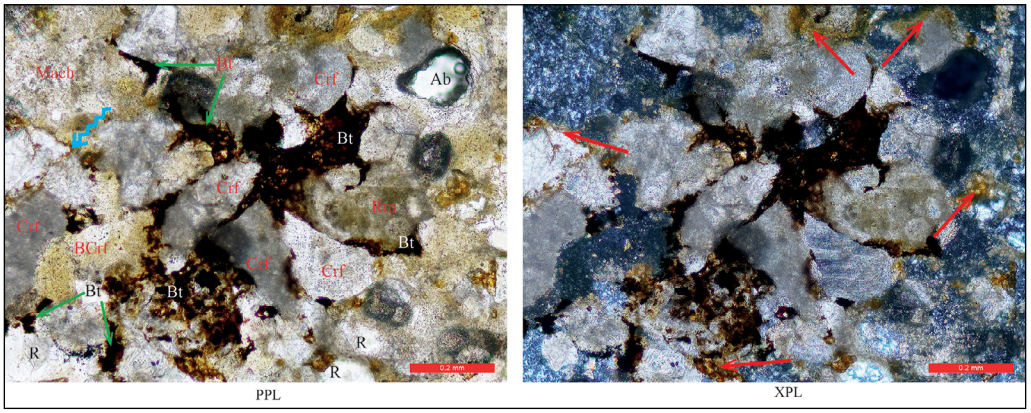

Figure 19- HL6-3. Mostly intergranular and little intragranular (lower left part of the center in this image) pores were blocked by bitumen fillings (Bt). Tangential, concavo convex and sutured grain contact types indicate tightly packing and high compaction. Note the moderately sorted and very angular to subangular grains.

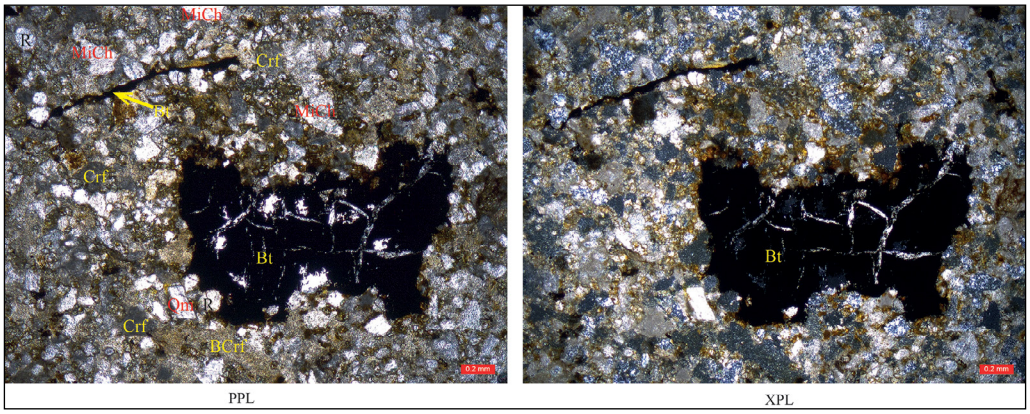

Figure 20- HL6-7. Microfractures in the solid bitumen were filled by calcite. Relative timing between the calcite fillings and bitumen shows that bitumen filled in pores before calcite, the fractures don't cut the section throughout, only limited in the bitumen filling. This relation indicates that the fractures occured after bitumen became solid then the calcite filled into the fractures. Monocrystalline quarts with fully extinction to the left down of the bitumen. To the top left a microfracture is filled by bitumen. Subangular to subrounded Crf and very angular lithic chert fragments are the dominant constitutes in this section.

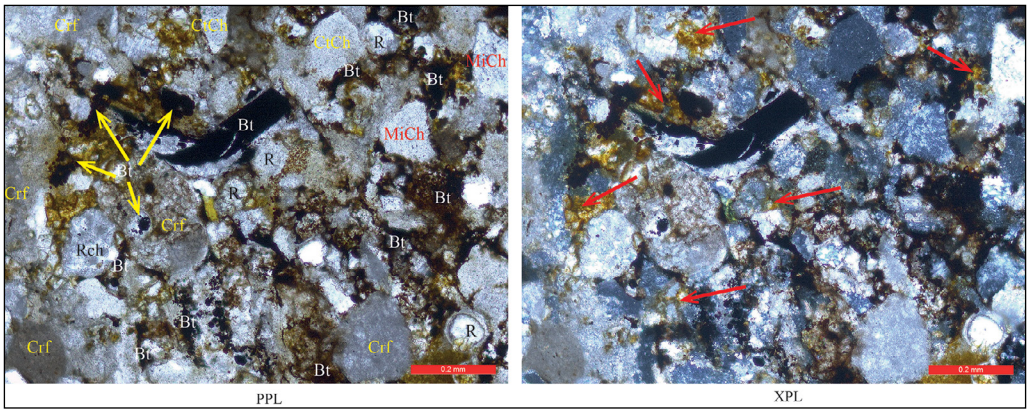

Figure 21- HL6-7. Majority of the intergranular and intragranular pore spaces filled by solid bitumen before or syn-calcite precipitation while the sandstone had pretty much pore spaces during early diagenesis. At that time the turbidite sandstones of Tanjero Formation had a good porosity which filled by solid bitumen since oil migration.

Both the provenance ternary diagram and the composition of the turbidite sandstones of Tanjero Formation in the studied area point out sedimentary rocks as source area. Taking together into account the petrographic and palaeoflow data (Table 1, and 2) (Figures 24 and 25) it is possible to consider only one source area composed of deep marine and shallow marine sedimentary rocks to the north as the main responsible for the composition of sandstones.

Lithic clast types in the petrographic composition of the sandstones represent the sedimentary rock types of the Lower Cretaceous Qulqula (radiolarian) Formation consisting of deep marine radiolarian sedimentary rocks and Balambo Formation composed of shallow marine limestone and shales supporting the basin by such asneritic transported broken fossil shells, glauconite grains, and undefinable fossils in the altered carbonate rock clasts,located in the lowermost part of the stratigraphic column of the northern Iraq region.

The reason for the absence of ophiolite fragments in thin sections is in contrast to the palaeogeographic drawings in previous works (e.g. Ameen, 2008; Karim and Taha, 2009; Karim and Surdashy, 2005*b*). This suggests that in the source area feeding the turbidites in the study area, the ophiolites do not crop out.

All the data from provenance analysis and petrography in this study show that provenance is not changing during deposition of the sandstones for

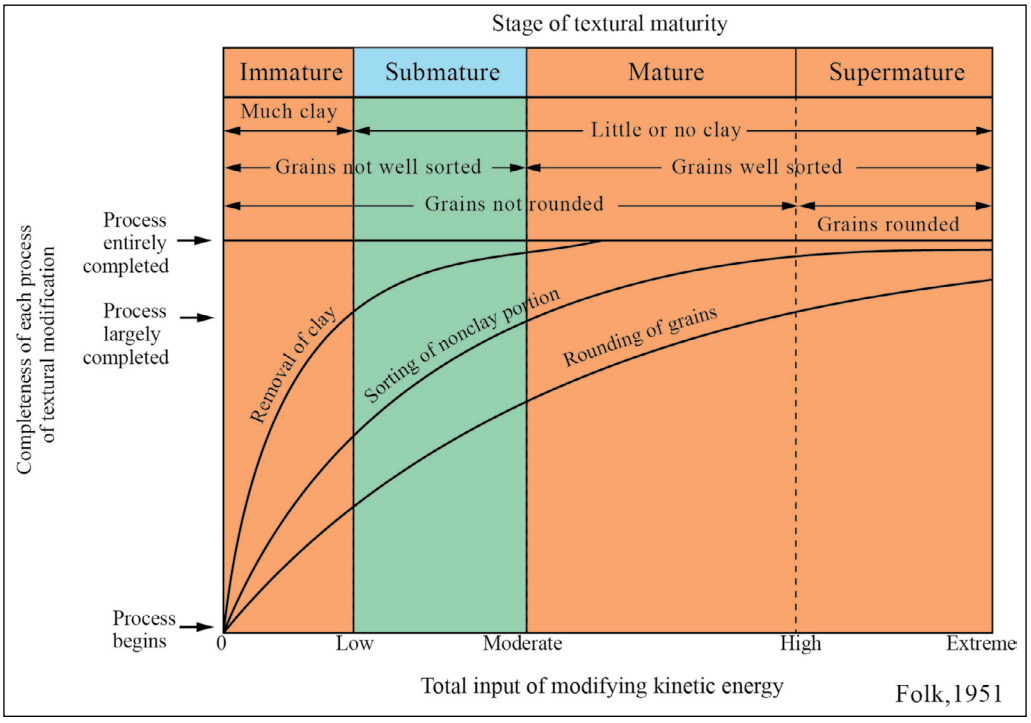

Figure 22- Turbidite sandstones of Tanjero Formation in the studied area indicate submature stage in the Folk's (1951) textural maturity table. Since as can be seen in table 1 and photomicrographs, there is no clay matrix in the sandstones, clay content of the turbidites is less than 5 %; poorly sorted; grains are not rounded.

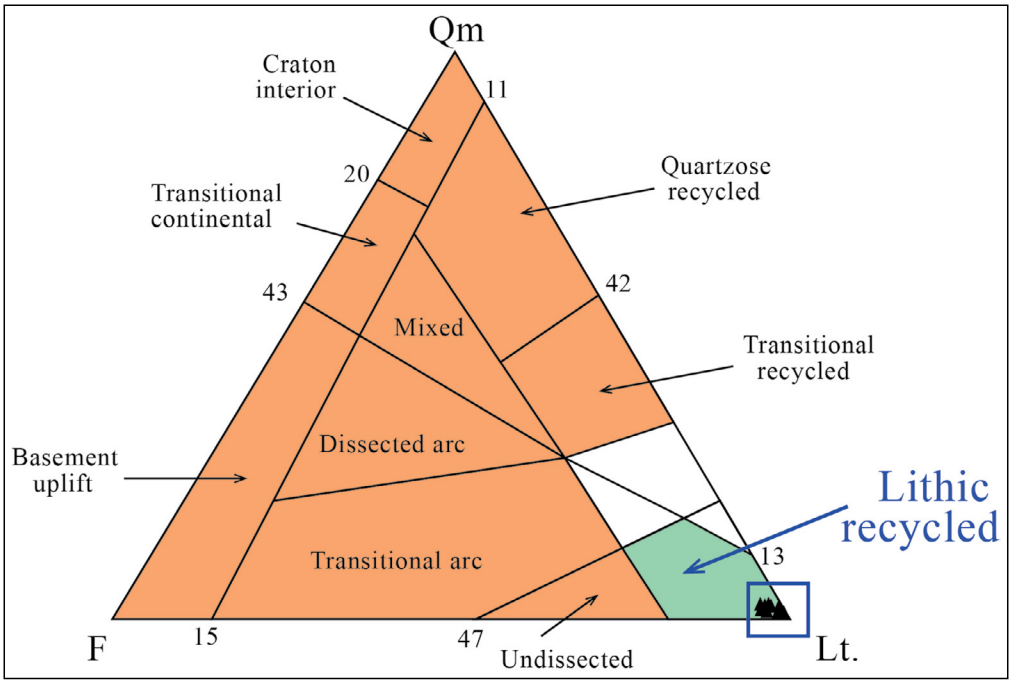

Figure 23- Qm-F-Lt ternary diagram showing tectonic provenance of the sandstones indicates "lithic recycled" category. Position of the samples in the Lt corner is exaggerated to make it visible (Dickinson et al., 1983).

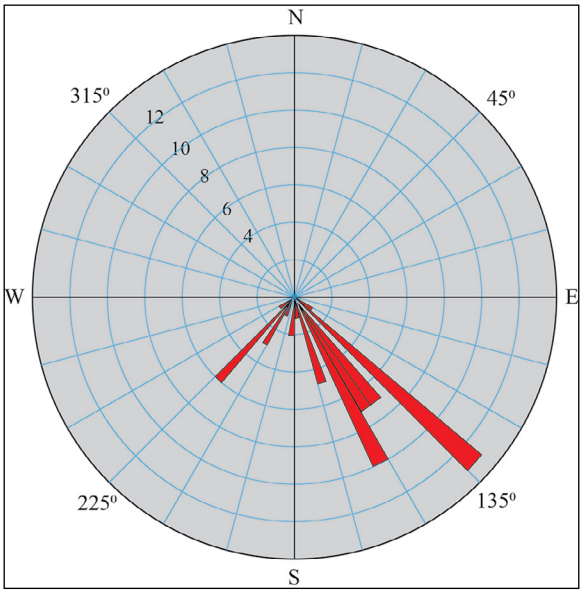

Figure 24- Rose diagram showing unidirectional palaeoflow of Tanjero Formation in the study area. Mean direction is toward south east.

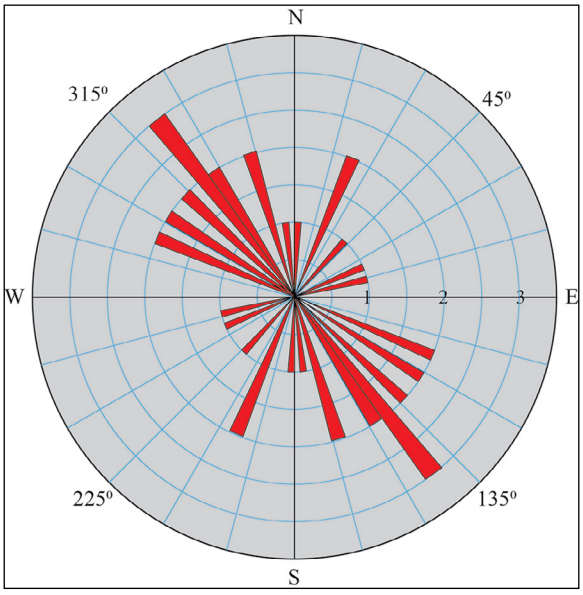

Figure 25- Rose diagram from bidirectional palaeoflow indicators shows Northwest – Southeast.

the studied area because of the average calclithite sandstone composition is not varying along the measured sections.

The results for provenance analysis in this study show different source area than the interpretations in Karim's studies in 2004, 2007 and 2010 as it is suggested that the source rock is only Qulqula Formation in his studies because of not sufficient petrographic analysis.

6. Palaeoflow Analysis

Previously two researchers, as in the following paragraphs, studied on palaeoflow direction of Tanjero Formation. They used many sedimentary structures, channel and incised valleys for indicating the direction in different places of northern Iraq.

Al-Rawi (1981) used flute casts, groove casts, ripple mark and cross beddingwith N45ºW and N85ºW in Dokan area and N45ºW in Sulaimaniyah area and concluded that the source area is in the East and the main direction of transport is toward northwest-west.

In Karim's (2004) study palaeo flow direction from ripple mark, elongate fossil, cross bedding, oriented plant fragments, imbricated pebbles, the direction of channel and incised valleys istoward south-outhwest in Sulaimaniyah and Darbandikhan area.

In this study 83 sedimentary structures (Table 2) in both types of unidirectional and bidirectional have been used to determine the direction of palaeoflow for Tanjero Formation.

6.1.Unidirectional Sedimentary Structures

Sixty-three unidirectional palaeo flow measurements, obtained from three types of sedimentary structures such as ripple mark, cross bedding and flute cast, show moderately southeast orientation (Figure 24). According to Potter and Pettijohn (1977) and Tucker (2011) there is a limit for tilt correction and they revealed that tilt below 30 degrees needs no correction.

6.2. Bidirectional Sedimentary Structures

Twenty measurements from oriented plant material, parting lineation and groove cast were in the rose diagram (Figure 25). The mean direction shows NW-SE.

Petrographic and palaeoflow analysis in this study pointed out that the source area is located moderately in the north and consisting of Lower Cretaceous (radiolarian) Qulqula and Balambo formations. The turbidity currents feeding the Tanjero Formation are initiating from the north than diverted to the south-east possibly depending on the basin plain topography

Table 2- Palaeoflow measurements from the seven measured sections.

No	Palaeoflow direction		Sedimentary structure	Bedding attitude		
				Dip angle	Dip direction (Azimuth)	Strike
Measurements from unidirectional sedimentary structures						
1	186		Ripple mark	24	66	156
2	164		Ripple mark	24	66	156
3	186		Ripple mark	24	66	156
4	134		Flute cast	24	66	156
5	208		Ripple mark	25	68	158
6	116		Ripple mark	25	68	158
7	144		Ripple mark	25	68	158
8	220		Ripple mark	25	68	158
9	168		Ripple mark	25	68	158
10	220		Ripple mark	25	68	158
11	220		Ripple mark	25	68	158
12	210		Ripple mark	25	68	158
13	220		Ripple mark	25	68	158
14	236		Ripple mark	25	68	158
15	230		Ripple mark	25	68	158
16	140		Ripple mark	25	68	158
17	180		Ripple mark	25	68	158
18	216		Ripple mark	23	50	140
19	220		Ripple mark	23	50	140
20	140		Ripple mark	23	50	140
21	150		Ripple mark	23	50	140
22	150		Ripple mark	23	50	140
23	150		Ripple mark	23	50	140
24	150		Ripple mark	23	50	140
25	160		Ripple mark	23	50	140
26	160		Ripple mark	23	50	140
27	128		Ripple mark	23	50	140
28	146		Ripple mark	23	50	140
29	160		Ripple mark	23	50	140
30	150		Ripple mark	23	50	140
31	180		Ripple mark	23	50	140
32	220		Ripple mark	24	68	158
33	148		Ripple mark	24	68	158
34	160		Ripple mark	24	68	158
35	210		Ripple mark	24	68	158
36	210		Ripple mark	24	68	158
37	145		Ripple mark	24	68	158
38	147		Ripple mark	24	68	158
39	144		Cross bedding	24	68	158
40	145		Ripple mark	24	68	158
41	149		Ripple mark	24	68	158
42	144		Ripple mark	24	68	158
43	148		Ripple mark	28	63	153
44	142		Ripple mark	28	63	153
45	134		Ripple mark	28	63	153
46	138		Ripple mark	28	63	153
47	134		Ripple mark	28	63	153
48	134		Ripple mark	28	63	153
49	140		Ripple mark	28	63	153
50	134		Ripple mark	29	50	140
51	134		Cross bedding	29	50	140
52	134		Cross bedding	29	50	140
53	134		Cross bedding	29	50	140
54	134		Cross bedding	29	50	140
55	134		Cross bedding	29	50	140
56	134		Cross bedding	29	50	140
57	134		Cross bedding	29	50	140
58	134		Ripple mark	29	50	140
59	150		Ripple mark	29	50	140
60	152		Ripple mark	29	50	140
61	152		Ripple mark	29	50	140
62	152		Ripple mark	29	50	140
63	152		Ripple mark	29	50	140
Measurements from bidirectional sedimentary structures						
1	170-350	350	Plant material	24	66	156
2	148-328	328	Parting lineation	24	66	156
3	130-310	310	Parting lineation	24	66	156
4	140-320	320	Parting lineation	24	66	156
5	164-344	344	Plant material	24	66	156
6	146-326	326	Plant material	25	68	158
7	112-292	292	Parting lineation	25	68	158
8	140-320	320	Plant material	25	68	158
9	78-258	258	Plant material	25	68	158
10	120-300	300	Plant material	25	68	158
11	132-312	312	Parting lineation	25	68	158
12	68-248	248	Parting lineation	25	68	158
13	40-220	220	Plant material	25	68	158
14	114-294	294	Plant material	25	68	158
15	120-300	300	Plant material	25	68	158
16	0-180	180	Groove cast	25	68	158
17	20-200	200	Plant material	23	50	140
18	160-340	340	Plant material	23	50	140
19	140-320	320	Plant material	23	50	140
20	22-202	202	Groove cast	29	50	140

and NW-SE directed basin margins during Late Cretaceous. In the studied area dip angle of beds are less than 30 degrees (Table 2 and Figure 26), because of that no needs to correction.

7. Discussion

The northern Iraq region is one of the largest oil accumulation field so far discovered in Iraq including some 50% (De Vera et al., 2009) of over 100 bn barrels (Iraq Oil and Gas Report Q1, 2018) mainly within the carbonate formations. The discovery of this and since the basin is located on the northern margin of the Arabian Plate, its tectonic evolution and collision with the Iranian Plate in along southern arm of the Neotethys ocean, led to vast amount of stratigraphic and tectonic national studies in the area mainly published in the national or regional journals that they are not international famous with little exception as given in the text and reference list in this paper. Additionally, the largest clastic turbidite unit on the geological map, Tanjero Formation, has not been petrographically studied yet as the main interest is on the carbonate units in the area for oil production. Also the political problems are the other important case that negatively affected sufficient international geological studies during the last decades.

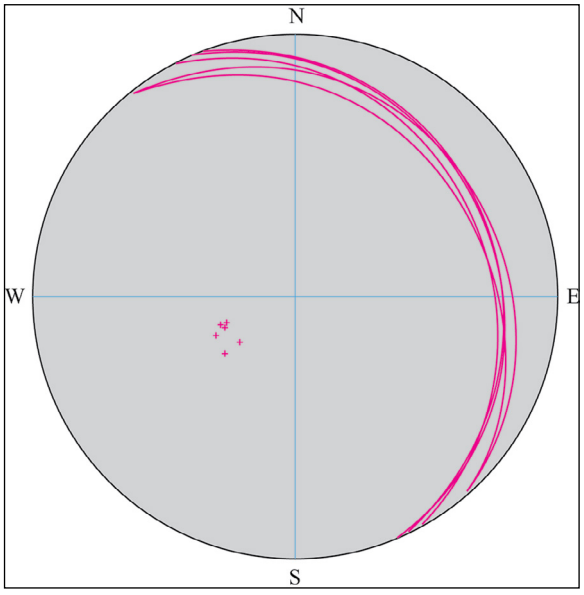

Figure 26- Stereonet showing bedding planes of sandstone in the studied area, dip angles are less than 30 degrees toward NE, plotted on the Geo Rose software.

For all that a consensus has not been reached yet on some of the subject such as the stratigraphic positions of many formations (etc. Red Bed Series, Qulqula Radiolarian Formation, Bekhme Formation), tectonic evolution and provenance for clastic rocks like Tanjero Formation since inadequate field and laboratory works. This study shows that these kind of controversial subjects like the gap on the provenance and related palaeogeographic evolution of the Tanjero Basin can be resolved successfully by a rigorous petrographic study which is open to international discussions and further studies in the other outcrops throughout on the unit.

Depositional history of the Cretaceous basin consisting of Tanjero Formation has been subjected to the following studies as illustrated in the figures 27, 28, 29 and 30. Qulqula Radiolarian Formation is the only

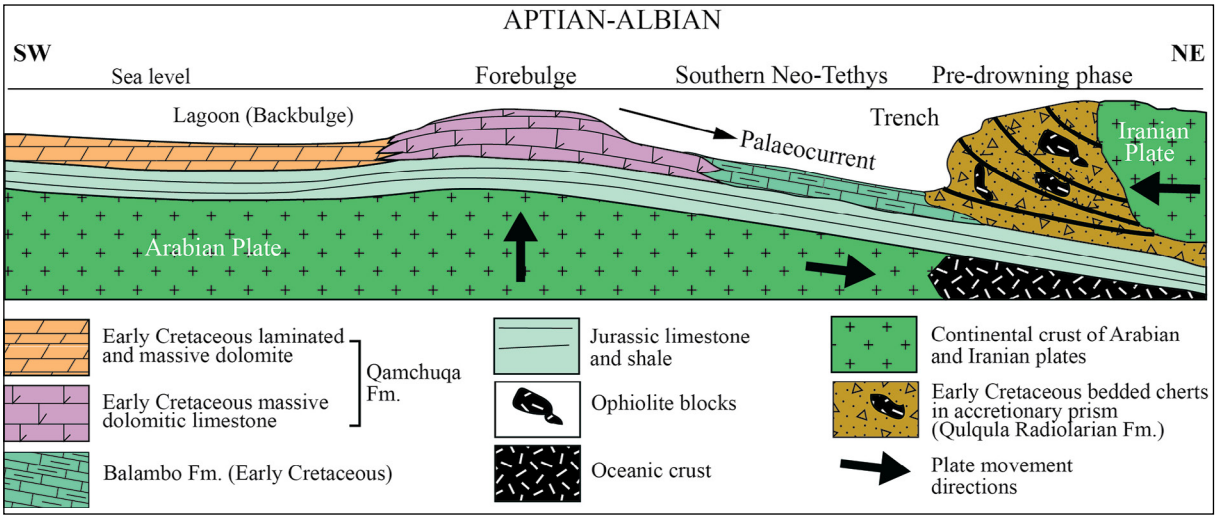

Figure 27- Depositional history of Early Cretaceous basin in which Qamchuqa and Balambo and Qulqula Radiolarite Formations are deposited (Ameen, 2008).

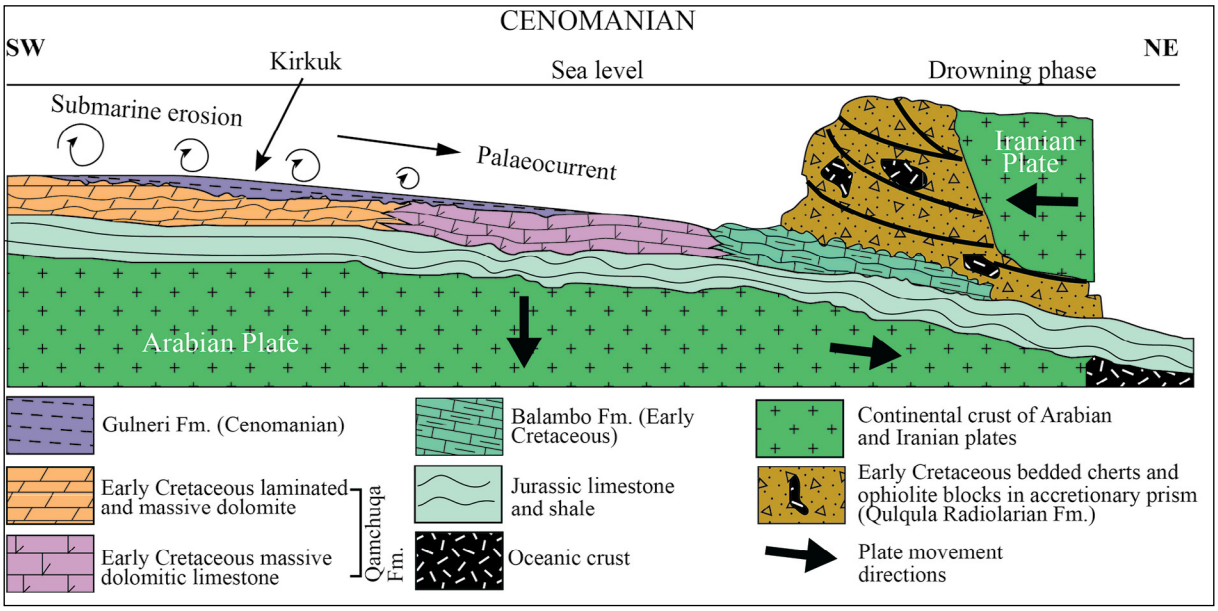

Figure 28- Tectonic and depositional model of the Late Cretaceous (Cenomanian) basin in which Kometan is deposited (Karim and Taha, 2009).

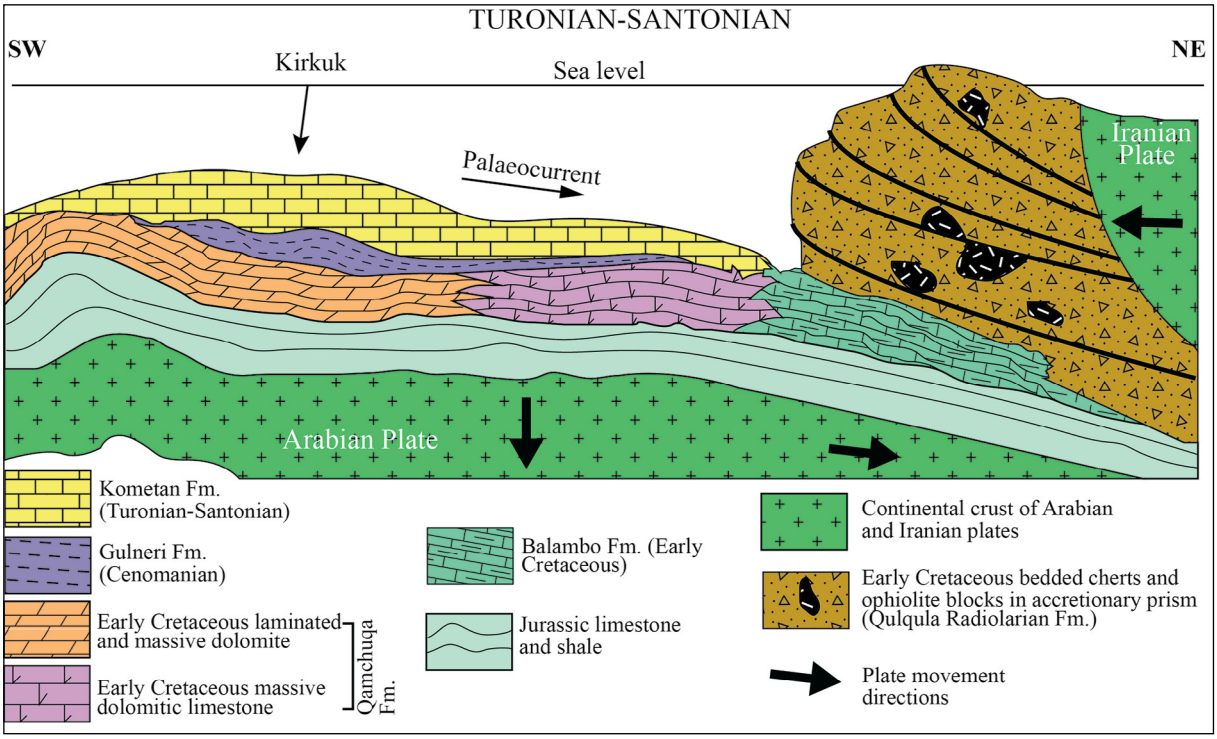

Figure 29- Tectonic and depositional model of the Late Cretaceous (Turonian-Campanian) basin in which Kometan and Bekhme Formation are deposited (Karim and Taha, 2009).

source rocks in these tectonic evolution models on the northern margin of the basin feeding Shiranish and Tanjero formations and the Red Bed Series. Balambo Formation is located under the accretionary prism and overthrusted Qulqula Radiolarian Formation so it doesn't crop out anywhere to be a source for the basin.

During Early Cretaceous under the load of the trench materials, the Arabian plate is suffered from flexure which is formed fore bulge. On this palaeo high Qamchuqa Formation is deposited as reefal and lagoonal sediments (Figure 27) (Ameen, 2008). The Kometan Formation is deposited after drowning of

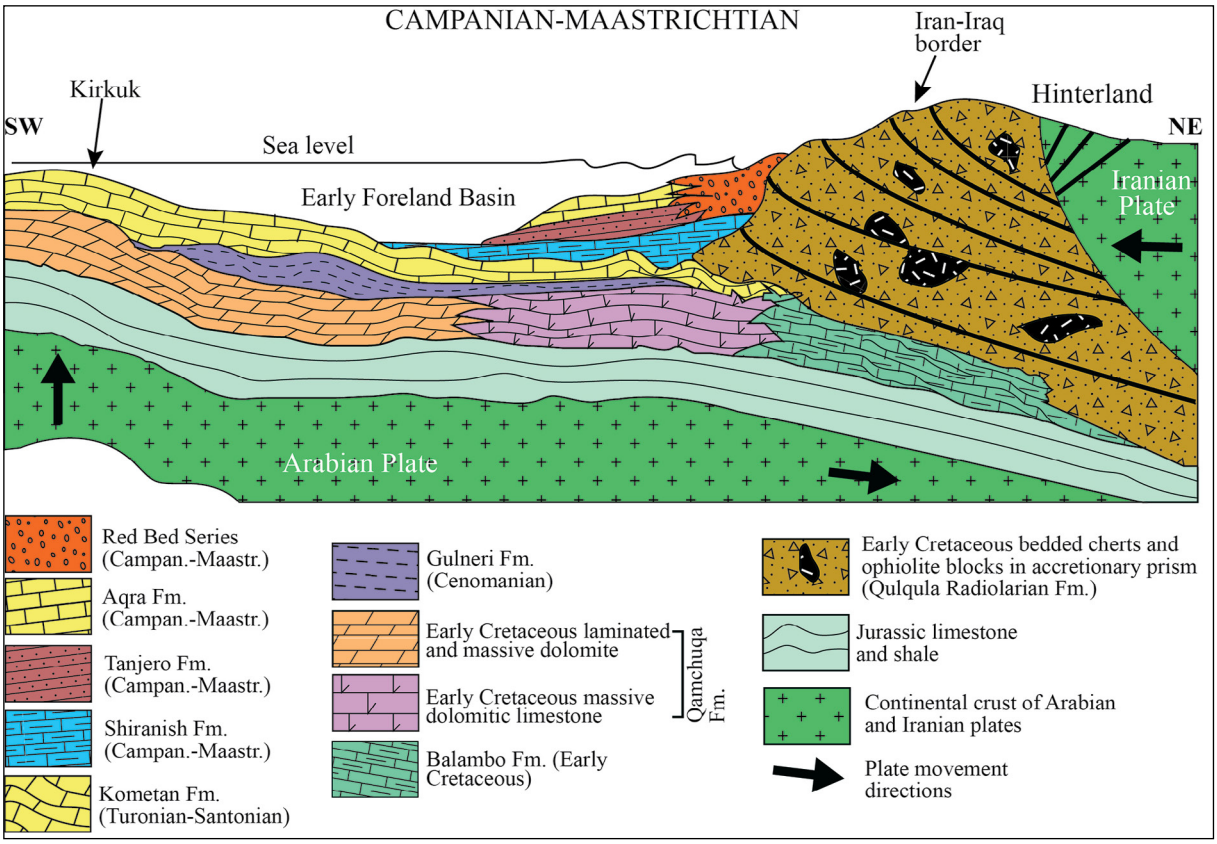

Figure 30- Combination of tectonic and depositional setting of Late Cretaceous basin in which Shiranish and Tanjero Formation are deposited (Karim and Surdashy, 2005*b*).

the Arabian Platform (Qamchuqa Formation) under the load of the trench material (accretionary prism materials) and Iranian plate in Cenomanian. The fore bulge is subsided and during subsiding Dokan and Gulneri formations are deposited as transitional facies, as sediments of intermediate depth between shallow (Qamchuqa) and deep (Kometan) during Turonian-Campanian (Figure 28) (Karim and Taha, 2009).

The Kometan Formation is deposited after drowning of the Arabian Platform Qamchuqa Formation under the load of the both accretionary prism materials and the Iranian plate, fore bulge subsided. The palaeocurrent was toward northeast. On this fore bulge, Qamchuqa Formation is deposited. Combination of tectonic and depositional setting of Late Cretaceous basin in which Kometan is deposited in Turonian-Campanian (Figure 29) (Karim and Taha, 2009).

During late Campanian the continental parts of the Iranian and Arabian plates are collided. The accretionary materials are pushed on to the Arabian Platform. Due to this collision a terrestrial land had generated the palaeocurrent is reversed toward southwest. In addition to that a foreland basin is formed in front of the Iranian Plate in which Shiranish and Tanjero formations are deposited (Figure 29) (Karim and Taha, 2009).

Qulqula Radiolarian Formation is a radiolaria fossils bearing deep marine sedimentary unit as seen in the tectonic models above and in the text and figure 2 and 3. In this study, petrographic analysis (Table 1, and the photomicrographs) shows that the modal composition of the turbidite sandstone of Tanjero Formation consisting of 59.2 % carbonate rock clastsin average and has some neritic fossil shell fragments. This result requires at least one carbonate unit in the source area. Due to the alteration on the carbonate rock fragments in the thin sections it is difficult to identify the fossils on the clasts and the hosting source rocks. Qamchuqa Formation mainly consisting of dolomitic limestonebut Tanjero Formation doesn't have any dolomitic clast representing Qamchuqa Formation (Figures 2 and 3). Balambo Formation is thought to

be the second source formation thrusted by Qulqula Radiolarian Formation must be located together in the accretionary prism which is not exist in the previous studies like in figure 28, 29 and 30.

As a result, the palaeogeographic evolution models must include Balambo Formation too at the northern side of the Cretaceous depositional environment as source area which is not in the previous models. This result contributes a new finding for the palaeogeographic evolution of the northern Iraq region.

8. Conclusions

It was determined that the Tanjero Formation consists of low density turbidites containing different parts of the Bouma sequence and that high density turbidites identified by Lowe (1982), usually represented by conglomerates, are not seen in this area. The reason for this was thought to be due to the presence of distal fan sediments in the study area, according to facies and facies associations.

The compositional characteristics show the presence of only sedimentary rocks in the source areas. Petrographic modal analysis of the thin sections of the sandstone fall into the calclithite area of litharenite division.

Very little amount of tangential, mainly long grain, concavo convex and sutured contact types and high contact index (4.7) represent moderate to tightly packing, moderate compaction. Less than 5 percentage clay, very fine to medium grained in size consisting of chert, siltstone, mudstone, radiolarian chert and radiolarian mudstone fragments, glauconite, neritic fossil shell fragments, fossil bearing carbonate rock clasts and angular to subangular in shape, very poorly to moderately sorted, transported over short distances are represented by submature stage.

Both the sandstone composition and the palaeoflow data indicating the flow towards the SE, measured from current ripples in Bouma Tc division and flute marks, and petrographic constituent of the sandstone point out a lithic recycle orogen category for the turbidite. This source area is the structural highs of the north of the Upper Cretaceous basin consisting of Lower Cretaceous (radiolarian) Qulqula and Balambo formations.

It was determined that the ophiolitic masses indicated in the previous studies as blocks within the accretionary prism did not constitute a source area for the turbidites of the Tanjero Formation widely exhumed around Sulaimaniyah.

Acknowledgements

The authors would like to thank to Professor Dr. Polla Azad Khanaqa head of the Institute for Strategic Studies and Scientific Researchin Sulaimaniyah, Iraq, for his hospitality, valuable advices on security and the preparation of the thin sections in the laboratory of the institute.We also wish to thank two anonymous reviewers for the time spent on this manuscript; their comments and suggestions have made significant improvements to the work.

References

Abdel Kireem, M. R. 1986*a*. Contribution to the Stratigraphy of the Upper Cretaceous and Lower Tertiary of the Sulaimaniyah - Dokan Region, Northeastern Iraq. Neues Jahrbuch Für Geologie Und Paläontologie – Abhandlungen 172 (1), 121-139.

Abdel Kireem, M. R. 1986*b*. Planctonic Foraminifera and stratigraphy of the Tanjero Formation (Maastrichtian), northeastern Iraq. Micropaleontology 32, 215-231.

Al Mehaidi, H.M. 1975. Tertiary nappe in Mawat range, NE Iraq. Geological Society of Iraq 8, 31 - 44.

Al Rawi, I. 1981. Sedimentology and Petrology of Tanjero Clastic Formation in north and northeastern Iraq. Unpublished Ph. D. Thesis, University of Baghdad, 295.

Alavi, M. 2004. Regional stratigraphy of the Zagros fold-thrust belt of Iran and its proforeland evolution. American Journal of Science 304, 1-20.

Alavi, M. 2007. Structures of the Zagros fold-thrust belt in Iran. American Journal of Science 307, 1067-1095.

Ameen, B.M. 2008. Lithostratigraphy and Sedimentology of Qamchuqa Formation from, NE Iraq. Unpublished Ph. D. Thesis. University of Sulaimani 147p.

Armas, P., Moreno, C., Sánchez, M.L., González, F. 2014. Sedimentary palaeoenvironment, petrography, provenance and diagenetic inference of the Anacleto Formation in the Neuquén Basin, Late Cretaceous, Argentina. Journal of South American Earth Sciences 53, 59-76.

Bellen, R.C.V., Dunnington, H.V., Wetzel, R., Morton, D.M. 1959. Lexique. Stratigraphique International, Asie Paris.

Bordy, E.M., Hancox, J.P., Rubidge, B.S. 2004. Provenance studies of the late Triassicearly Jurassic Elliot formation, main Karoo Basin, South Africa. Geological Society of South Africa.South African Journal of Geology 107, 587-602, 59-76.

Buday, T., Jassim, S.Z. 1987. The Regional geology of Iraq: Tectonism Magmatism, and Metamorphism. In: M. J. Abbas and Jassim, S. Z (Ed.). Geosurvey, Baghdad, Iraq, 445.

Cingolani, C.A., Manassero, M., Abre, P. 2003. Composition, provenance and tectonic setting of Ordovician siliciclastic rocks in the San Rafael block: southern extension of the Precordillera crustal fragment, Argentina. Journal of South American Earth Science 16, 91-106.

Çelik, H, Salih, T.M.H. 2018. Provenance investigation from sedimentary petrography of the Upper Cretaceous deep marine low density turbidites of the Tanjero Formation around Arbat, northeastern Iraq. Turkish Journal of Earth Sciences 27 (6), 432-459.

De Vera, J., Gines, J., Oehlers, M., McClay, K., Doski, J. 2009. Structure of The Zagros fold and thrust belt in the, northern Iraq. Trabajos de Geología, Universidad de Oviedo 29, 213-217.

Dickinson, W.R. 1970. Interpreting detrital modes of greywacke and arkose. Journal of Sedimentary Research 40, 695–707.

Dickinson, W.R. 1988. Provenance and sediment dispersal in relation to paleotectonics and paleogeography of sedimentary basins. In: Kleinspehn KL, Poala C, editors. New Perspectives in Basin Analysis. New York, NY, USA: Springer, pp. 3-25.

Dickinson, W.R., Suczek, C. 1979. Plate tectonics and sandstone composition. American Association of Petroleum Geologist Bulletin 63, 2164-2194.

Dickinson, W.R., Beard, S., Brakenbridge, F., Erjavec, J., Fergusion, R., Inman, K., Knepp, R., Linberg, P., Ryberg, P. 1983. Provenance of the North American Phanerozoic sandstones in relation to tectonic setting. Geological Society of America Bulletin 64, 222-235.

Dunnington, H.V. 1958. Generation, Migration and Dissipation of Oil in northern Iraq. Arabian Gulf, Geology and Productivity. American Association of Petroleum Geologist Foreign Reprint Series No. 2.

Folk, R.L. 1951. Stages of textural maturity in sedimentary rocks. Journal of Sedimentary Petrology 21,127–130.

Folk, R.L. 1966. A review of grain-size parameters. Sedimentology 6, 73-93.

Gazzi, P. 1966. Le arenarie del flysch sopracretaceo dell'Appennino modenese; correlazioni conil flysch di Monghidoro: Mineralogische und Petrographische Acta 12, p 69–97.

Ghosh, S., Sarkar, S., Ghosh, P.2012. Petrography and major element geochemistry of the Permo-Triassic sandstones, central India: implications for provenance in an intracratonic pull-apart basin. Journal of Asian Earth Sciences 43(1), 207–240.

Iraq Oil and Gas Report Q1. 2018. Includes 10-Year Forecasts to 2026. BMI Research, A Fitch Group Company. https://www.bmiresearch.com.

Jaza, I. 1992. Sedimentary facies analysis of the Tanjero Clastic Formation in Sulaimaniyah District, northeast Iraq. Unpublished MSc. Thesis, Salahaddin University, 121.

Johnson. M.R. 1976. Stratigraphy and Sedimentology of the Cape and Karoo Sequences in the Eastern Cape. Ph.D. Thesis (Unpublished). Rhodes University, Grahams town, South Africa 1-267.

Karim, K.H. 2004. Basin Analysis of Tanjero Formation in Sulaimaniyah Area, NE-Iraq. PhD. Thesis.

Karim, K.H. 2007. Possible effect of storm on sediments of Upper Cretaceous Foreland Basin: a case study for tempestite in Tanjero Formation, Sulaimanyia Area, NE-Iraq. Iraqi Journal of Earth Science 7, 1-10.

Karim, K.H. 2010. Modification of the time-expanded stratigraphic column of North East Iraq during Cretaceous and Tertiary. Published in: Petroleum Geology of Iraq (First Symposium, 21-22 April, Baghdad, Abstract book, 4.

Karim, K.H., Surdashy, A.M. 2005*a*. Palaeocurrent analysis of Upper Cretaceous Foreland basin a case study for Tanjero Formation in Sulaimaniyah area, NE-Iraq, 2005. Iraqi Journal of Earth Science 5, 30-44.

Karim, K.H., Surdashy, A.M. 2005*b*. Tectonic and depositional history of Upper Cretaceous Tanjero Formation in Sulaimaniyah area, NE-Iraq. Journal of Zankoi Sulaimani 8, 47-62.

Karim, K.H., Taha, Z.A. 2009. Tectonical history of Arabian platform during Late Cretaceous an example from NE Iraq. Iranian Journal of Earth Sciences 1, 1-14.

Karim, K.H., Al-Hamadani, R.K., Ahmad, S.H. 2012. Relations between Deep and Shallow Stratigraphic Units of northern Iraq during Cretaceous. Iranian Journal of Earth Sciences 4, 95-103.

Karim, K.H., Ismail, K.M., Bziany, M.M. 2014. Origin of Fossiliferous Limestone Beds inside the Upper Part of Tanjero Formation at the Northwest of Sulaimaniyah Area, NE Iraq. Journal of Zankoi Sulaimaniyah 17, 155-165.

Kassab, I.I.M. 1975. Planktonic Foraminifera Range in the type Tanjero Formation Upper Campanian-Maastrichtian) of N. Iraq. Geological Society of Iraq 8, 73 - 86.

Koshnaw, R.I., Stockli, D.F., Schlunegger, F. 2018. Timing of the Arabia-Eurasia continental collision—Evidence from detrital zircon U-Pb geochronology of the Red Bed Series strata of the northwest Zagros hinterland, K. region of Iraq. Geology 47: 47-50.

Koshnaw, R.I., Horton, B.K., Stockli, D.F., Barber, D.E., Tamar-Agha, M.Y. 2019. Sediment routing in the Zagros foreland basin: Drainage reorganization and a shift from axial to transverse sediment dispersal in the northern Iraq Basin Research 00: 1-28.

Lawa, F.A., Koyi, H., Ibrahim, A. 2013. Tectono-Stratigraphic Evolution of The NW Segment of the Zagros Fold-Thrust Belt, NE Iraq. Journal of Petroleum Geology 36 (1), 75-96.

Lawa, F.A., Al-Karadakhi, A.I., Ismail, K.M. 2017. An interfingering of the Upper Cretaceous rocks from Chwarta-Mawat Region (NE-Iraq). Iraqi Bulletin of Geology and Mining 13 (1), 15-26.

Li, G., Pe-Piper, G., Piper, D.J.W. 2012. The provenance of Middle Jurassic sandstones in the Scotian Basin: petrographic evidence of passive margin tectonics. Canadian Journal of Earth Sciences 49, 1463–1477.

Lowe, D.R. 1982. Sediment gravity flows: II. Depositional models with special reference to the deposits of high-density turbidity currents. Journal of Sedimentology 52, 279-297.

Malekzade, Z., Bellier, O., Abbassi, M.R., Shabanian, E., Authemayou, C. 2016. The effects of plate margin inhomogeneity on the deformation pattern within West-Central Zagros Fold-and-Thrust Belt. Tectonophysics 693, 304–326.

Mange, M.A., Morton, A.C. 2007. Geochemistry of heavy minerals. In Heavy Minerals in Use. Edited by M. Mange, and D.K. Wright. Developments in Sedimentology 58, 345–391.

Minas, H. 1997. Sequence stratigraphic analysis of the Upper Cretaceous succession of Central and northern Iraq. Unpublished PhD. Thesis, University of Baghdad. 188.

Moradpour, A., Sahamieh, R.Z., Khalaji, A.A., Sarikhani, R. 2017. Textural records and geochemistry of the Kermanshah mantle peridotites (Iran): implications for the tectonic evolution of southern Neo-Tethys. Journal of Geosciences 62, 165–186.

Motaghi, K., Shabanian, E., Tatar, M., Cuffaro, M., Doglioni, C. 2017. The south Zagros suture zone in tele seismic images. Tectonophysics 694, 292–301.

Pettijohn, F.J., Potter, P.E., Siever, R. 1987. Sand and Sandstone. Second edition. Springer -Verlag. New York Inc. New York. 553.

Potter, P.E., Pettijohn, F.J. 1977. Palaeocurrent and Basin Analysis, second ed., 413. Springer-Verlag, Berlin.

Raymond, L.A. 1995. The Study of Igneous, Sedimentary and Metamorphic Rocks. Wm.C. Brown Communication Inc., United States of America, 264-388.

Rieser, A.B., Neubauer, F., Liu, Y., Ge, X. 2005. Sandstone Provenance of north-western sectors of the intracontinental Cenozoic Qaidam basin, western China: Tectonic Vs Climatic control. Journal of Sedimentary Geology 177, 1–18.

Sharbazheri, K.M. 2007. Aging of unconformity within Tanjero Formation in Chwarta Area Northeast of Iraq. Iraqi Journal of Earth Science 7, 37-54.

Sharbazheri, K.M. 2010. Planktonic foraminiferal biostratigraphy of the upper Cretaceous reddish to pale brown transitional succession in Smaquli area, northeast Iraq. Iraqi Bulletin of Geology and Mining 6, 1-20.

Sissakian, V.K. 2013. Geological evolution of the Iraqi Mesopotamia Foredeep, inner platform and near surroundings of the Arabian Plate. Journal of Asian Earth Sciences 72, 152–163.

Sissakian, V.K., Fouad, S.F. 2015. Geological Map of Sulaimaniyah Quadrangle, at scale of 1: 250 000. Journal of Zankoi Sulaimani Part-A- Pure and Applied Sciences.

Tucker, M.E. 2011. Sedimentary rocks in the field: A practical guide. 4th edn. A John Wiley and Sons Ltd. Publication, 276. ISBN: 978-0-470-68916-5.